



HAL
open science

Stratigraphic Relationships in Jezero Crater, Mars: Constraints on the Timing of Fluvial-Lacustrine Activity From Orbital Observations

S. Holm-Alwmark, K. M. Kinch, M. D. Hansen, S. Shahrzad, K. Svennevig,
W. J. Abbey, R. B. Anderson, F. J. Calef, S. Gupta, E. Hauber, et al.

► **To cite this version:**

S. Holm-Alwmark, K. M. Kinch, M. D. Hansen, S. Shahrzad, K. Svennevig, et al.. Stratigraphic Relationships in Jezero Crater, Mars: Constraints on the Timing of Fluvial-Lacustrine Activity From Orbital Observations. *Journal of Geophysical Research. Planets*, 2021, 126, 10.1029/2021JE006840 . insu-03710145

HAL Id: insu-03710145

<https://insu.hal.science/insu-03710145>

Submitted on 30 Jun 2022

HAL is a multi-disciplinary open access archive for the deposit and dissemination of scientific research documents, whether they are published or not. The documents may come from teaching and research institutions in France or abroad, or from public or private research centers.

L'archive ouverte pluridisciplinaire **HAL**, est destinée au dépôt et à la diffusion de documents scientifiques de niveau recherche, publiés ou non, émanant des établissements d'enseignement et de recherche français ou étrangers, des laboratoires publics ou privés.



Distributed under a Creative Commons Attribution 4.0 International License

Key Points:

- We have studied stratigraphic relations between geologic units in Jezero crater for determination of relative age relations in the crater
- Topographic profiles and digital elevation models indicate that the western delta is on top of the youngest crater floor unit(s)
- We thus place constraints on the timeline of fluvial-lacustrine activity in Jezero crater

Correspondence to:

S. Holm-Alwmark,
sanna.alwmark@nbi.ku.dk

Citation:

Holm-Alwmark, S., Kinch, K. M., Hansen, M. D., Shahrzad, S., Svennevig, K., Abbey, W. J., et al. (2021). Stratigraphic relationships in Jezero crater, Mars: Constraints on the timing of fluvial-lacustrine activity from orbital observations. *Journal of Geophysical Research: Planets*, 126, e2021JE006840. <https://doi.org/10.1029/2021JE006840>

Received 23 JAN 2021
 Accepted 8 JUN 2021

© 2021. The Authors.

This is an open access article under the terms of the [Creative Commons Attribution-NonCommercial-NoDerivs License](#), which permits use and distribution in any medium, provided the original work is properly cited, the use is non-commercial and no modifications or adaptations are made.

Stratigraphic Relationships in Jezero Crater, Mars: Constraints on the Timing of Fluvial-Lacustrine Activity From Orbital Observations

S. Holm-Alwmark^{1,2,3} , K. M. Kinch¹ , M. D. Hansen¹, S. Shahrzad⁴, K. Svennevig⁵ , W. J. Abbey⁶, R. B. Anderson⁷ , F. J. Calef III⁶ , S. Gupta⁸, E. Hauber⁹ , B. H. N. Horgan¹⁰ , L. C. Kah¹¹ , J. Knade⁹, N. B. Miklusickak¹¹, K. M. Stack⁶, V. Z. Sun⁶ , J. D. Tarnas⁶, and C. Quantin-Nataf¹²

¹Niels Bohr Institute, University of Copenhagen, Copenhagen, Denmark, ²Natural History Museum Denmark, University of Copenhagen, Copenhagen, Denmark, ³Department of Geology, Lund University, Lund, Sweden, ⁴School of Earth and Environment, University of Leeds, Leeds, UK, ⁵Geological Survey of Denmark and Greenland, Copenhagen, Denmark, ⁶Jet Propulsion Laboratory, California Institute of Technology, Pasadena, CA, USA, ⁷U.S. Geological Survey, Astrogeology Center, Flagstaff, AZ, USA, ⁸Department of Earth Science and Engineering, Imperial College London, London, UK, ⁹German Aerospace Center, Institute of Planetary Research, Berlin, Germany, ¹⁰Department of Earth, Atmospheric, and Planetary Sciences, Purdue University, West Lafayette, IN, USA, ¹¹Department of Earth and Planetary Sciences, University of Tennessee-Knoxville, Knoxville, TN, USA, ¹²Laboratoire de Géologie de Lyon -Terre, Planètes, Environnement, University of Lyon, Lyon, France

Abstract On February 18, 2021 NASA's Perseverance rover landed in Jezero crater, located at the northwestern edge of the Isidis basin on Mars. The uppermost surface of the present-day crater floor is dominated by a distinct geologic assemblage previously referred to as the dark-toned floor. It consists of a smooth, dark-toned unit overlying and variably covering light-toned, roughly eroded deposits showing evidence of discrete layers. In this study, we investigated the stratigraphic relations between materials that comprise this assemblage, the main western delta deposit, as well as isolated mesas located east of the main delta body that potentially represent delta remnants. A more detailed classification and differentiation of crater floor units in Jezero and determination of their relative ages is vital for the understanding of the geologic evolution of the crater system, and determination of the potential timeline and environments of habitability. We have investigated unit contacts using topographic profiles and DEMs as well as the distribution of small craters and fractures on the youngest portions of the crater floor. Our results indicate that at least some of the deltaic deposition in Jezero postdates emplacement of the uppermost surface of the crater floor assemblage. The inferred age of the floor assemblage can therefore help to constrain the timing of the Jezero fluvio-lacustrine system, wherein at least some lake activity postdates the age of the uppermost crater floor. We present hypotheses that can be tested by Perseverance and can be used to advance our knowledge of the geologic evolution of the area.

Plain Language Summary On February 18, 2021 NASA's Perseverance rover landed in Jezero crater on Mars. In the past, the crater was filled with water, forming a lake, and in the western part of the crater an ancient delta is preserved. Part of the present-day crater floor has been interpreted to represent a lava flow that was deposited after the lake dried out, meaning that the floor unit would be younger than the western delta. In order to understand how the Jezero crater lake has developed over time, including the potential timeline and environments of habitability, it is necessary to work out the relations between the geologic units in Jezero crater. In this work, we have analyzed orbital images of Jezero crater and reveal how the crater floor and delta deposits relate to each other in time. Our results show that at least some of the deltaic deposits in Jezero overlie the youngest crater floor unit(s). It is therefore possible to learn broadly when fluvial activity in the crater has been effective from the age of the crater floor. Our work presents hypotheses that can be tested by Perseverance to advance our knowledge of how the area has evolved geologically over time.

1. Introduction

Jezero crater is the landing site for the Mars 2020 Perseverance rover mission. The Perseverance rover, which landed on Mars on February 18, represents the first step in a multimission program to collect, cache, and return samples from Mars to Earth (Farley et al., 2020). The crater is ~45 km in diameter and located at the northwestern edge of the Isidis basin, in the Nili Fossae region of Mars (at 18.4°N, 77.7°E; Figure 1; e.g., Bramble et al., 2017; Ehlmann, Mustard, Fassett, et al., 2008; Ehlmann, Mustard, Murchie, et al., 2008; Fassett & Head, 2005; Goudge et al., 2015, 2017; Scheller & Ehlmann, 2020; Stack et al., 2020). The presence of an inlet valley entering the crater and an outlet valley exiting the crater, together with the preservation of a fluvial deltaic sedimentary body (the western delta) at the mouth of the inlet valley implies a prolonged history of lacustrine activity within the crater (Figures 1c and 2; e.g., Fassett & Head, 2005; Goudge

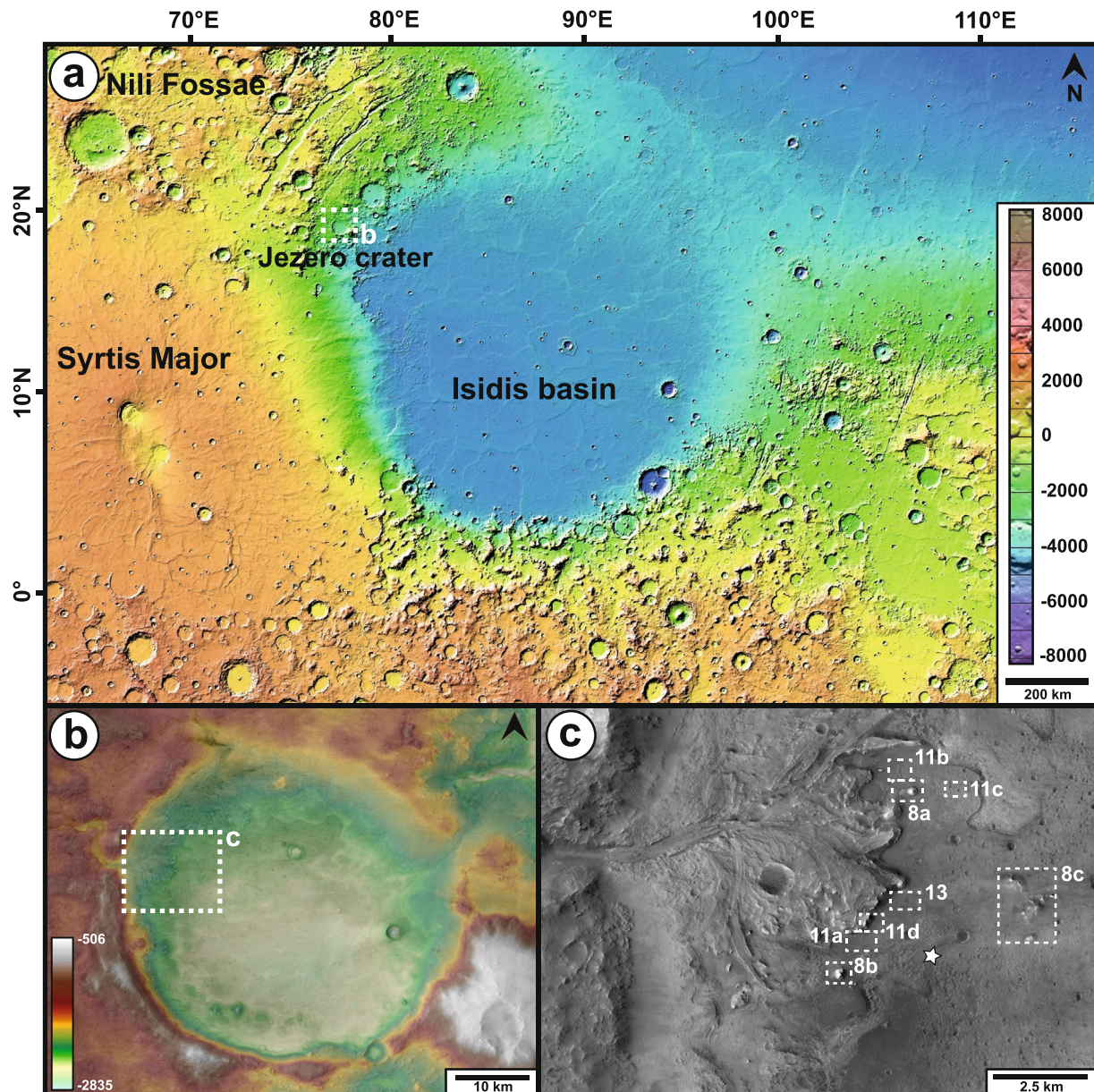


Figure 1. (a) Regional overview map with MOLA elevation data (elevation in meters) of the area where Jezero crater is located (credit USGS Astrogeology Science Center, Goddard Space Flight Center, NASA; https://planetarymaps.usgs.gov/mosaic/Mars_MGS_MOLA_ClrShade_merge_global_463m.tif). Elevation in meters. (b) Color-coded elevation image of Jezero crater based on HRSC DEM and corresponding orthoimages. All elevations (in m) below Mars's areoid. (c) HiRISE image mosaic close-up of the study area (Ferguson, Galuszka, et al., 2020) with the Perseverance landing site marked with a star.

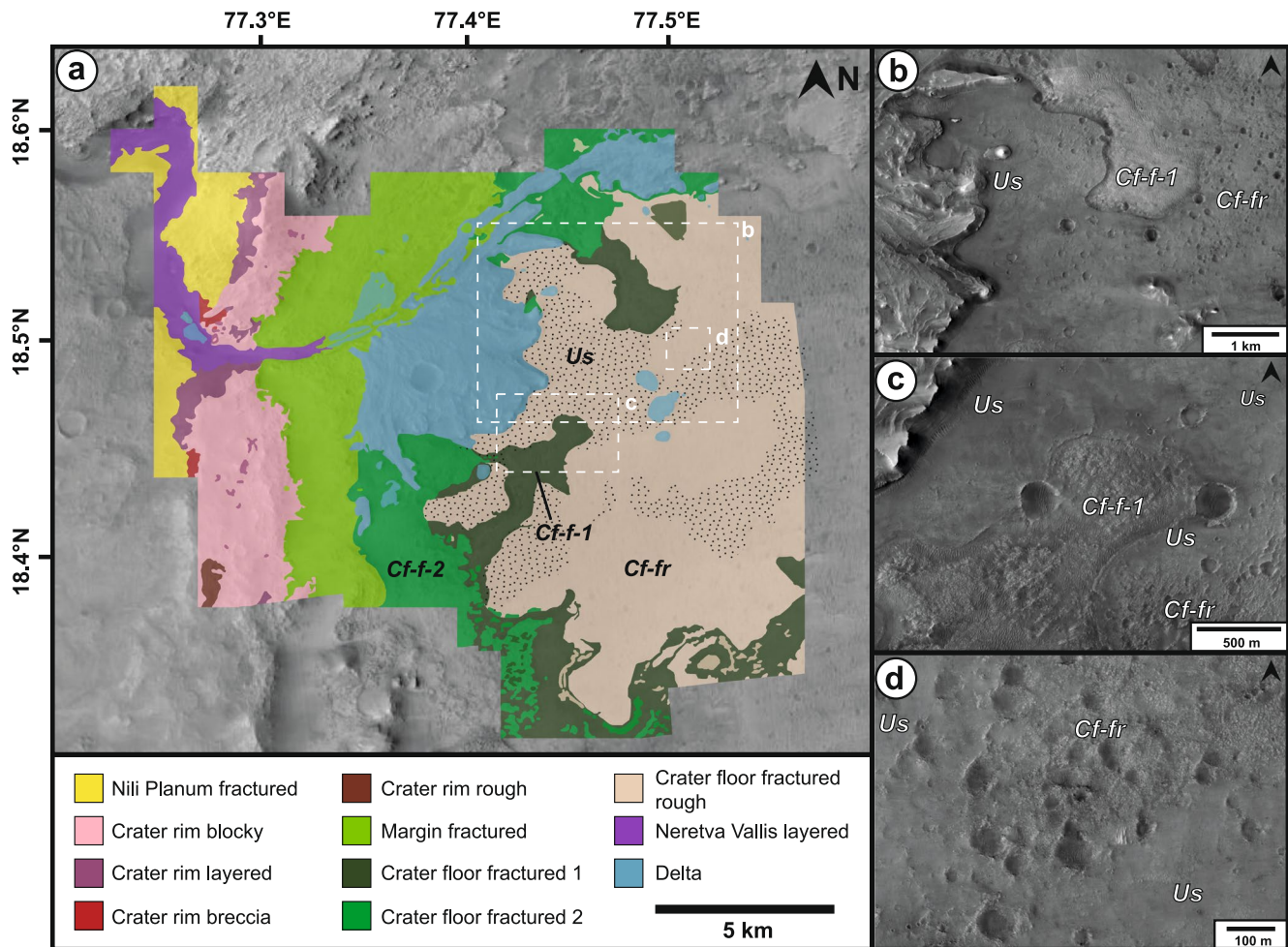


Figure 2. (a) Photogeologic map showing bedrock units and surficial cover of the undifferentiated smooth (Us) unit on the crater floor fractured rough unit in the study area in Jezero crater. Note that the Us unit is a surficial unit that mantles bedrock in the map area of Stack et al. (2020), e.g., on the crater rim, on the western delta, and on the crater floor but that this map only shows the extent of the most prominent cover of Us on the Cf-fr unit, as this is the focus of this study. Note the higher-standing blue features, possible delta remnants, here referred to as delta-associated remnant deposits, to the east of the main delta body. Units discussed in this paper are Cf-f-1: crater floor fractured 1, Cf-f-2: crater floor fractured 2, Cf-fr: crater floor fractured rough, Us: undifferentiated smooth. Figure modified after Stack et al. (2020). Us unit extent after Sun and Stack (2020b). (b–d) Surface expression of the Cf-f-1, Cf-fr, and Us units in Jezero crater. HiRISE image mosaic base (Ferguson, Galuszka, et al., 2020). HiRISE, High Resolution Imaging Science Experiment.

et al., 2015, 2017; Mangold et al., 2020; Salese, Kleinhans, et al., 2020; Schon et al., 2012; Stack et al., 2020). Additional sedimentary fan deposits present in the northern part of the crater are highly eroded and it is presently not clear whether those deposits are alluvial or deltaic in origin, to what extent deposits are linked to the western delta, or to what extent they may represent a discrete delta linked to a northern river inlet (e.g., Goudge et al., 2015; Horgan et al., 2020; Salese, Kleinhans, et al., 2020; Schon et al., 2012).

Understanding the timing of deposition of sedimentary units in Jezero crater is vital to the understanding of both hydrological and geologic history of the region, with broader implications for the entire planet. Jezero crater contains a series of geomorphic/geologic units, including discrete, identifiable subunits, that are distributed across the original crater floor (Table 1 and Figure 2; Stack et al., 2020). Investigation of contacts relations and the relative elevation of these discrete subunits permits a first-order hypothesis of the organization of the stratigraphy—and therefore the relative age—of the subunits (Stack et al., 2020). Identified units include three morphologically distinct rough fractured units [crater floor fractured 1 (Cf-f-1), crater floor fractured 2 (Cf-f-2), and crater floor fractured rough (Cf-fr)], and an undifferentiated smooth unit (Us; Figures 2 and 3). Us is a surficial unit that is interpreted to mantle bedrock in the map area of Stack et al. (2020), e.g., on the crater rim, within and on the western delta in Jezero, and on the crater floor.

Table 1

Nomenclature of Crater-Fill Units in Jezero Used in This Study and Comparison With That Used in Examples of Older Literature

Unit (this work; after Stack et al., 2020)	Schon et al. (2012)	Goudge et al. (2015)	Shahrzad et al. (2019)	Horgan et al. (2020)	Sun and Stack (2020b)	Warner, Schuyler, et al. (2020)
Undifferentiated smooth (US)					Dark mantle	Regolith
Crater floor fractured rough (Cf-fr)	Volcanic unit	Volcanic floor unit	Dark-toned (mafic) floor	Mafic floor	Jezero floor unit	Mafic floor unit
Crater floor fractured 1 (Cf-f-1)					Lower etched	—
Crater floor fractured 2 (Cf-f-2)	Basin fill	Light-toned floor unit	Light-toned floor unit	Light-toned floor unit	Upper etched	—

Although Us units mapped by Stack et al. (2020) generally have uniform textures and tones (at map scale), these deposits were likely not all deposited at the same time, are not comprised of the same material or deposited in the same environment (Stack et al., 2020). Relations observed during detailed mapping suggests that, in all cases, deposition/formation of the Us unit postdates deposition of the rough fractured units (Kah et al., 2020; Stack et al., 2020; Warner, Schuyler, et al., 2020); the stratigraphic relationships among differentiated rough fractured units, however, remains poorly constrained.

In previous studies, units identified here as Cf-fr and Us had been interpreted as a single, highly crater-retaining unit (e.g., “volcanic floor unit,” “dark-toned mafic floor;” Goudge et al., 2015; Shahrzad et al., 2019), which has allowed previous authors to determine its age through crater counting. Although crater-counting ages have varied widely, from 3.45 Ga (Goudge et al., 2015) to 1.4 Ga (Schon et al., 2012), more recent works (Shahrzad et al., 2019; Warner, Schuyler, et al., 2020) provide strong arguments for an early Amazonian age [2.6 ± 0.5 Ga; Shahrzad et al., 2019, 2.3 ± 0.2 Ga; Warner, Schuyler, et al., 2020; see also discussion in Marchi (2021)]. In light of current mapping, we should remember that the 2.6 and 2.3 Ga dates represents crater counting on a surface composed of two stratigraphically distinct subunits. That is, the Us is interpreted as a dark mantling unit that variably drapes the surface of the light-toned Cf-fr unit by Stack et al. (2020; Figures 2 and 3). Warner, Schuyler, et al. (2020b) interpreted the smooth upper subunit of the Cf-fr [corresponding to Us in Stack et al. (2020)] in their study area in the center of the crater as a regolith. Crater counting on in the central area of Jezero (Warner, Schuyler, et al., 2020) indicate that the surface is not at equilibrium with surface processes, as 20–70 m craters are being eroded faster than they are produced, and recent work (Quantin-Nataf et al., 2021) highlights spatial variation in the distribution of craters on the floor unit in Jezero, of the sizes that were counted by Shahrzad et al. (2019). Quantin-Nataf et al. (2021) showed that the youngest crater floor unit has a complex history of cover and later exhumation, complicating interpretation of the crater statistics on the surface.

The aim of this study is to characterize the stratigraphic relations between the youngest crater floor units in Jezero crater (Cf-fr and Us), the western delta stratigraphic units, and a set of possible remnant deposits forming isolated mesas close to the western delta scarp that may represent lacustrine or deltaic deposits associated with the main delta (Figure 2). According to the interpretation that the dark floor unit (Cf-fr + Us) represents the youngest deposits (Goudge et al., 2015) inside of the crater, their emplacement age would also define the timing of when fluvial activity inside Jezero crater ceased. We show how our new observations can be used to place more robust temporal constraints on geologic events that characterize Jezero crater. Finally, investigating specific features that modify units that make up the Jezero crater floor (e.g., crater density distribution and the distribution of fractures), we extend our understanding of the origin of crater floor units, and present detailed hypotheses that can be tested using the Perseverance rover.

2. Background and Geological Setting

The timing and nature of fluvial activity on Mars have been intensely debated (Kite, 2019; Palumbo et al., 2020, and references therein). Studies of a variety of Martian valley networks, e.g., Craddock and Howard (2002), Howard, Craddock and Moore, (2005), Hoke and Hynes (2009), Hynes et al. (2010), Davis et al. (2016), and Salese, McMahon, et al. (2020) strongly suggest an active hydrologic cycle with prolonged periods of precipitation, suggesting a different climate on Mars in the past. Although the nature of the

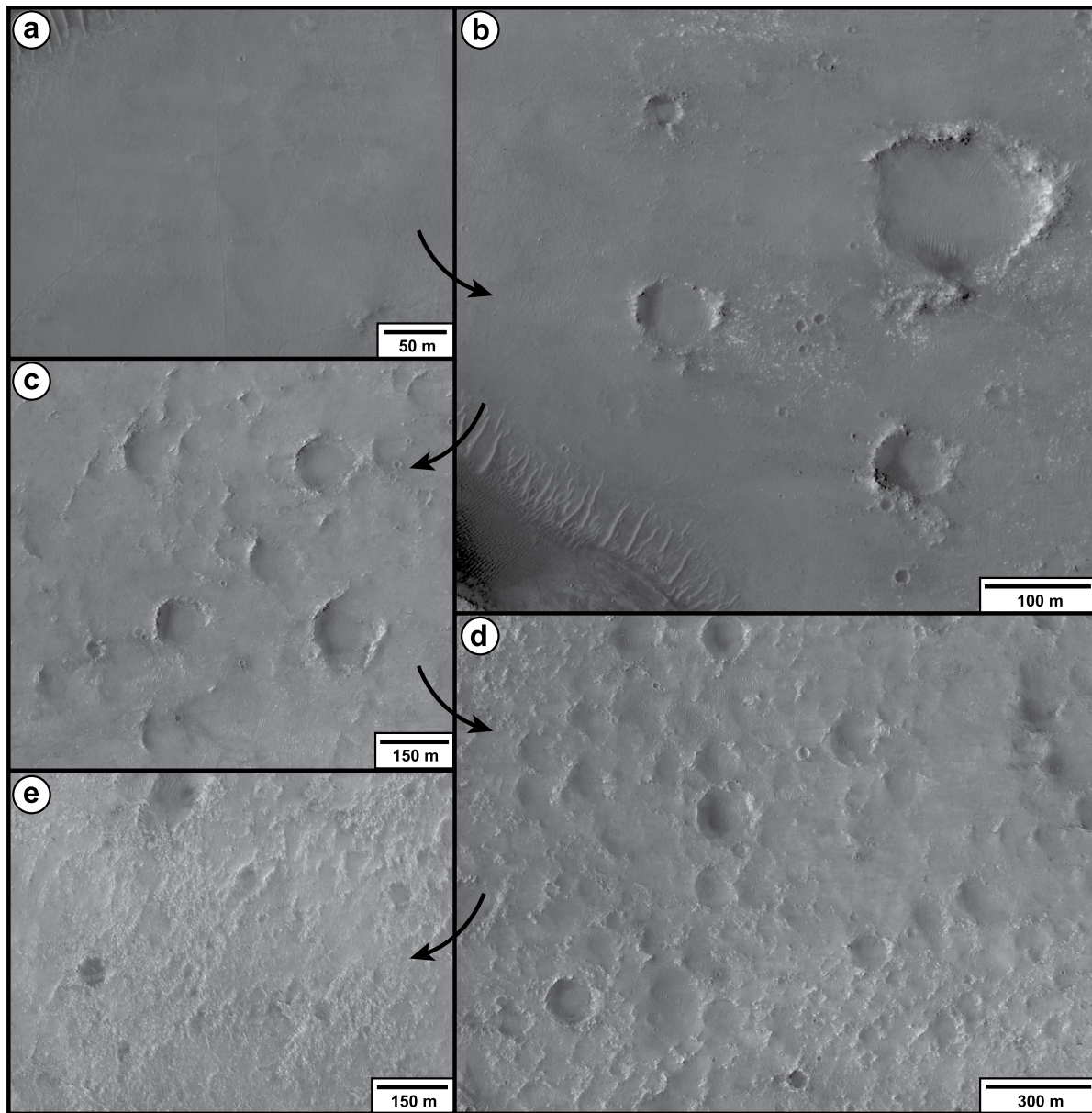


Figure 3. Close-up on HiRISE images (Ferguson, Galuszka, et al., 2020) showing surface expression of the Us and Cf-fr units in Jezero crater, with decreasing mantling (or presence of) the Us unit (highlighted by direction of arrows). (a) Smooth texture of the Us unit. (b) Transition from smooth Us-dominated surface to heavily mantled Cf-fr unit. (c) Mantled. (d) Less mantling of Cf-fr unit with rough texture and crater retaining. (e) Rough texture of Cf-fr and with relatively poor retention of craters and crater rims. North is up in all images. HiRISE, High Resolution Imaging Science Experiment.

ancient Mars climate remains contested, e.g., Carr and Head (2003), and Howard et al. (2005), have proposed that rapid melting of snow or ice could produce discharges consistent with valley network morphologies in the absence of a more traditional, warm fluvial system. Grau Galofre et al. (2020) recently suggested that the majority of valley networks are a result of combined surface and subglacial runoff, relaxing the requirement for warm surface conditions on the wet, ancient Mars. Regardless, such observations require an atmosphere on Mars capable of maintaining an active hydrologic cycle that included water that was stable on the surface.

Jezero crater is inferred to have maintained a standing body of water associated with a time of ongoing fluvial activity on Mars (Fassett & Head, 2008b). During this period, fluvial input along the western, and potentially northern, margins of the crater supplied drainage of surficial fluids from the surrounding regions

(e.g., Mangold et al., 2020; Salese, Kleinhans, et al., 2020, and references therein); an outlet channel on the eastern margin of Jezero may have resulted in episodic draining of the crater lake (Holo & Kite, 2017; Salese et al., 2019; Salese, Kleinhans, et al., 2020). The duration of deltaic deposition and the persistence of lacustrine activity in Jezero have been estimated to have occurred over several years to millions of years (Fassett & Head, 2005; Goudge et al., 2015; Lapôtre & Ielpi, 2020; Mangold et al., 2020; Salese et al., 2019; Salese, Kleinhans, et al., 2020; Schon et al., 2012). In terms of the timing of aqueous activity, Mangold et al. (2020) were unable to definitely determine an age of delta formation, but concluded that the latest delta-related deposits formed during a period of reactivation of the lower sections of the fluvial valley that fed the western delta in Jezero, and that this reactivation occurred sometime in the Late Noachian to Hesperian. Fluvial activity that carved the older, upper part of the valley likely commenced during the Middle Noachian (Mangold et al., 2020). Such an interpretation is consistent with observations from Irwin, Craddock, Howard (2005), and Howard, Craddock & Moore (2005), Fassett and Head (2008a), Hoke and Hynes (2009), and Mangold et al. (2020), who hypothesized that the majority of fluvial activity (and therefore paleolacustrine activity; Fassett & Head, 2008b) on Mars peaked around the Noachian-Hesperian boundary, and terminated soon thereafter. In the time since fluvial and lacustrine activity ended, most paleolake deposits, including those within Jezero, have experienced significant geological modification by processes that may include volcanism (Schon et al., 2012, and references therein), aeolian deposition, and erosion. Prior to the upcoming in-situ investigation of Jezero crater by the Perseverance rover and potential sample return, critical analysis of stratigraphic relationships in the surficial units of Jezero crater provides the best mechanism for building a stratigraphic and temporal framework.

The age of Jezero crater can be bracketed by the formation of the Isidis basin (3.96 ± 0.01 Ga; Werner, 2008) and the emplacement of a regional olivine-carbonate unit that is inferred to be younger than Jezero crater as it overlaps at least the northern rim of Jezero (3.82 ± 0.07 Ga; Goudge et al., 2015; Mandon et al., 2020), which places it in the Noachian period (see also Ehlmann et al., 2009; Goudge et al., 2015). The crater presently has a shallow depth profile compared to fresh Martian impact craters (Garvin et al., 2003; Schon et al., 2012). The shallow depth profile suggests substantial crater-fill deposited on top of the original crater floor, which has an estimated thickness of about 1 km (Ehlmann, Mustard, Fassett, et al., 2008; Schon et al., 2012). These deposits would be expected to include a combination of different materials, including impact ejecta, volcanic deposits, lacustrine sediments, alluvial sediments, and aeolian deposits that cover the primary impactites (if not previously removed by erosion) and the entire central uplift of the crater. Using scaling relationships presented by Whitehead et al. (2010), the height of the central uplift of Jezero can be estimated to 0.33 km (if crater diameter is 45 km), although it should be noted that central uplift height relative to diameter of crater has been shown to vary greatly on Mars [see, e.g., discussion in Calef et al. (2016)].

2.1. Crater-Fill Units

In this study, we follow the naming scheme defined by Stack et al. (2020; see also Figure 2). Table 1 summarizes the relevant units with the names used in this study, as well as names employed by a number of previous authors.

All crater-fill units in Jezero crater may have a more complicated history than would be inferred by continuous deposition inside of the crater following the law of superposition. Following evidence from other craters (e.g., Gale crater, Malin & Edgett, 2000; Watkins et al., 2016), deposits may have been buried and then later exhumed (see also Quantin-Nataf et al., 2021; Warner, Schuyler, et al., 2020), and the stratigraphic succession in the crater is likely to contain a number of local to regional unconformities (Stack et al., 2020). It is also possible that the units that can be observed from orbit may represent complex lateral interfingering facies rather than traditional “layer cake” deposition (Stack et al., 2020). The units that are recognized as exposed Jezero crater floor are described below.

2.1.1. Crater Floor Fractured 1 and 2

Units Cf-f-1 and Cf-f-2 (Figure 2) are massive, light-toned units with meter-scale fractures. The contact between the two is gradational. Stack et al. (2020) distinguishes the topographically higher Cf-f-2 from the lower Cf-f-1 primarily by elevation, but also by the presence of small bumps and ridges that gives Cf-f-2

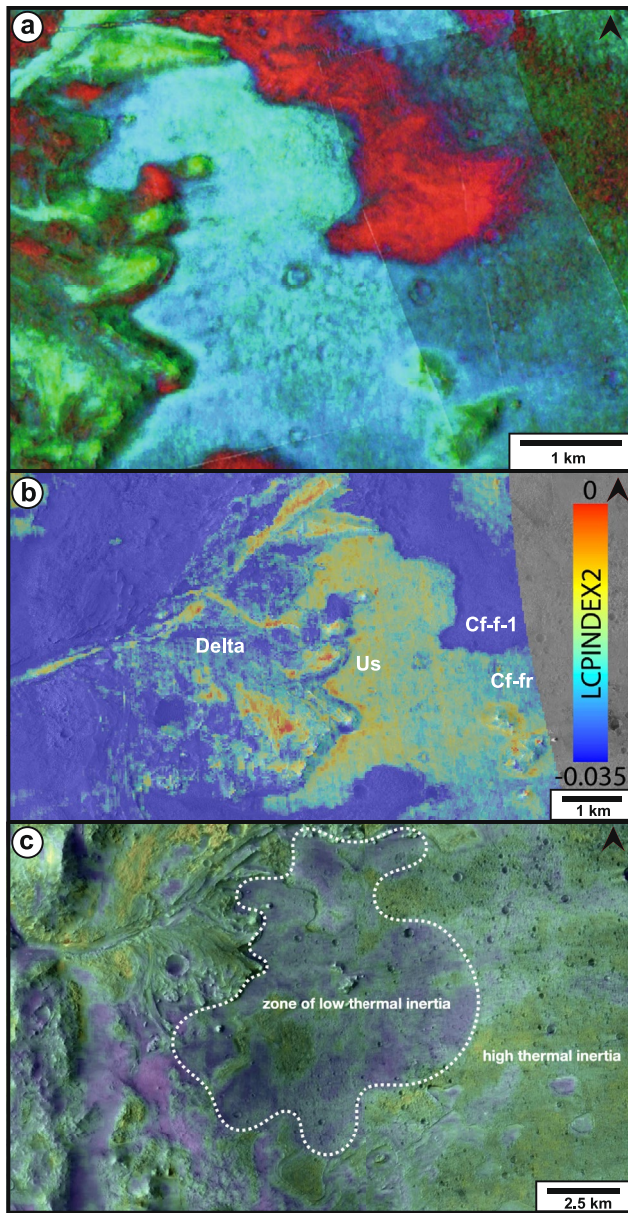


Figure 4. (a) Mafic spectral signatures from primary minerals showing mineralogical differences between the delta, the Cf-fr + Us, and Cf-f units. After Horgan et al. (2020). Green = low-calcium pyroxene, blue = high-calcium pyroxene, red = olivine and Fe-carbonates. Frame is the same as in Figure 2b. (b) Distribution of spectral signals consistent with low-calcium pyroxene in the western delta, crater floor units, and delta-associated deposits (blue is low, red is high). (c) THEMIS-derived thermal inertia map of part of Jezero crater. Note the general low thermal inertia of the area close to the western delta edge, where the Us unit is most prominent (see Ferguson et al., 2006).

a “pock-marked” texture. Previous publications (Goudge et al., 2015; Horgan et al., 2020), group the two units together as “light-toned floor” or “basin fill” (Schon et al., 2012). Cf-f-2 has textural and morphological similarities with the Cf-fr (described below), but Cf-f-2 is significantly less crater retaining than Cf-fr, at all crater scales. Spectrally, the Cf-f units both display olivine and carbonate signatures, and so they are not separated into two units by Horgan et al. (2020). The Cf-f units have been interpreted as either a crater-filling material that is unique to Jezero by Schon et al. (2012), or as part of the regionally extensive carbonate-bearing and olivine-bearing unit that is prevalent throughout the Isidis-Nili Fossae region (Brown et al., 2020; Goudge et al., 2012; Kremer et al., 2019; Mandon et al., 2020). Given that spectral signatures of the Cf-f units are broadly similar to those in the regional olivine-carbonate unit in the Jezero-area (Horgan et al., 2020), this indicates that there are two possible scenarios for the units (Horgan et al., 2020): either that they represent reworked sediments from the regional olivine-carbonate unit, or that they are the local expression of this regional unit.

2.1.2. Crater Floor Fractured Rough

Cf-fr is a crater-retaining unit interpreted as bedrock that is more resistant to erosion, and contains fractures at two distinct scales (fracture lengths of meters-and of several hundreds of meters; Stack et al., 2020). This unit has lobate margins and surrounds current and formerly higher-standing outcrops of Cf-f-1. It covers much of the Jezero crater floor, and is partially overlain by the Us unit, and appears to be underlain by Cf-f-1 (Stack et al., 2020). Previous workers have generally interpreted Cf-fr and the overlying smooth mantle (Us) as the same unit with the names “dark-toned floor,” “mafic floor,” and “volcanic floor” all employed by different authors (e.g., Goudge et al., 2015; Horgan et al., 2020; Schon et al., 2012; Shahrzad et al., 2019). The dark tone that has been associated with this unit, and led to the name “dark-toned floor, mafic floor” etc. (Table 1), is explained by Stack et al. (2020) as likely reflecting partial cover by a darker mantling unit (Us). Spectrally, the uppermost crater floor units (i.e., both Cf-fr and Us) are characterized by a high-calcium pyroxene (HCP) signal (Figure 4a; Horgan et al., 2020). The HCP signal is interpreted to be derived from the unit itself, in contrast to olivine-enriched streaks of sediment extending across the unit that are likely derived from the Cf-f units and low-calcium pyroxene (LCP) signal (Figure 4b) associated with deposition of material eroded from the western delta and delta-associated remnant deposits (Horgan et al., 2020).

There are a variety of depositional mechanisms proposed for the Cf-fr unit; igneous (e.g., Goudge et al., 2012, 2015; Schon et al., 2012) as well as fluvial or aeolian sedimentary (Kah et al., 2020; Stack et al., 2020). Several authors (e.g., Goudge et al., 2015; Horgan et al., 2020; Sun & Stack, 2020b) have suggested a potential correlation between the crater floor unit and a unit mapped outside of the crater, the Sun and Stack (2020b) Nili plains 2 unit and Bramble et al.’s (2017) mafic capping unit. If the Cf-fr unit is related to the geographically widespread Nili Planum capping unit (see also Hundal et al., 2020; Sun & Stack, 2020a, 2020b), the unit spans too large

a range in elevation for a volcanic flow to be a viable emplacement mechanism, whereas airfall deposition could explain the range in elevation (Sun & Stack, 2020a, 2020b).

A volcanic source for the Cf-fr (e.g., Goudge et al., 2012, 2015; Schon et al., 2012) was proposed based on the observations that the unit is topographically smooth and has a low regional slope; has lobate margins, high

thermal inertia, a high capacity to retain small craters; and has CRISM spectral signatures are consistent with volcanic rocks on Mars (Goudge et al., 2015; Horgan et al., 2020). Horgan et al. (2020) hypothesized that, if the unit is a locally sourced volcanic lava flow or tephra, the source could be either dikes and fissures in the crater floor that are covered by the unit or an enigmatic conical and cratered edifice located adjacent to the southeastern rim of Jezero. Crater retention and morphometry on the Cf-fr unit(s) indicate that the rock is resistant (Warner, Schuyler, et al., 2020). Warner, Schuyler, et al. (2020) compared their observations from Jezero with the resistant basaltic lava plain at the InSight landing site showing important similarities in crater morphology and time scales of erosion between the units, with one notable difference, the thickness of the regolith, and suggested that the Cf-fr unit is possibly igneous rock.

Other authors have suggested that a lack of textures expected from volcanic units on Mars such as platy textures or ridges (Golder, Miklusicak, et al., 2020), a variety of intermixed surface textures, the embayment of topographically high regions of crater fill, and enhanced mantling in regional topographic lows are more consistent with a different mode of formation, such as a low viscosity flow or by airfall/aeolian deposition [Golder, Miklusicak, et al., 2020; Grant & Schultz, 1990; Horgan et al., 2020; Kah et al., 2020; see also discussion in Stack et al. (2020)], and that many of these features may arise from a relation with dark-toned mantling material (i.e., the Us). It should be noted that the specific comparative textures lacking on the Cf-fr unit used in the analysis by Golder, Miklusicak, et al. (2020) are associated with Amazonian-aged lava flows (e.g., Golder, Burr & Kattenhorn, 2020; Jaeger et al., 2010; Keszthelyi et al., 2000), and primary volcanic textures are not expected to be preserved over time scales that are relevant here. In fact, Golder, Miklusicak, et al. (2020) noted that the textures on the unit were more similar to Hesperian to Noachian aged units in the Eridania basin. At the InSight landing site only vague flow boundaries, and no primary surface textures are associated with the basaltic material (the formation age of the smooth terrain covering the InSight landing ellipse is Early Amazonian; Warner, Grant, et al., 2020).

2.1.3. Undifferentiated Smooth Surface Cover

Us is a dark-toned mantling unit that overlies and drapes the Cf-fr unit. The unit is characterized by a relatively low thermal inertia (Figure 4c; see also Stack et al., 2020). The Us unit has a smooth upper surface and a complex relation with Cf-fr. Closer to the western delta deposit, the Us unit is inferred to be thicker, as the surface has a smoother appearance (Figures 2 and 3) that lacks lighter-toned rough textures and large craters (Stack et al., 2020). Stack et al. (2020) hypothesize that the unit may be a residual deposit from ash, aeolian, or residual accumulation of sand, pebbles, and cobbles left after deflation of the landscape. According to the hypothesis of Warner, Schuyler, et al. (2020), that the Us is a regolith at least in their investigated area in the center of Jezero, enhanced mantling in topographic lows could result from enhanced preservation of a smooth regolith in regions that are protected from wind deflation. According to this hypothesis, the larger-scale transition from smoother to rougher texture is caused by incomplete regolith deflation or exhumation of the Cf-fr unit. Areas of the Us unit with the smoothest appearance stand out as exhibiting clear CRISM spectral signatures of HCP (Figure 4a). Because HCP signatures are rare on the delta and absent in the Cf-f units, this may suggest a distinct source for Us materials (Horgan et al., 2020). There is also a low-calcium pyroxene (LCP) spectral signature on the Us, especially prominent on the area closest to the delta scarp (Figure 4b).

Variations in surface textures on the Cf-fr and Us units are most obvious when it comes to smoothness (Figures 2 and 3; see also, e.g., Golder, Miklusicak, et al., 2020; Kah et al., 2020; Stack et al., 2020). The smooth texture is most prominent close to the edge of the western delta, and the smooth regions grade into regions that expose progressively more of the underlying unit (Figure 3; see, e.g., Golder, Miklusicak, et al., 2020; Kah et al., 2020). Craters from the underlying unit are argued to be variably draped and show up as “ghost craters” as the Us gets thicker by Kah et al. (2020). Warner, Schuyler, et al. (2020), on the other hand, describe these as degraded features resulting from regolith development and aeolian infilling. Increased exposure of Cf-f1/2 unit is shown by CRISM signatures displaying stronger olivine signal and weaker pyroxene signals (Horgan et al., 2020; see also Figure 4a).

In this study, we analyzed features of the Cf-fr and Us units. Although these two units are clearly distinct, ambiguities regarding the complex relation between these units and the nature of both units hinder broad-scale interpretation. For discussion purposes, we follow earlier work (e.g., Goudge et al., 2015; Shahrzad

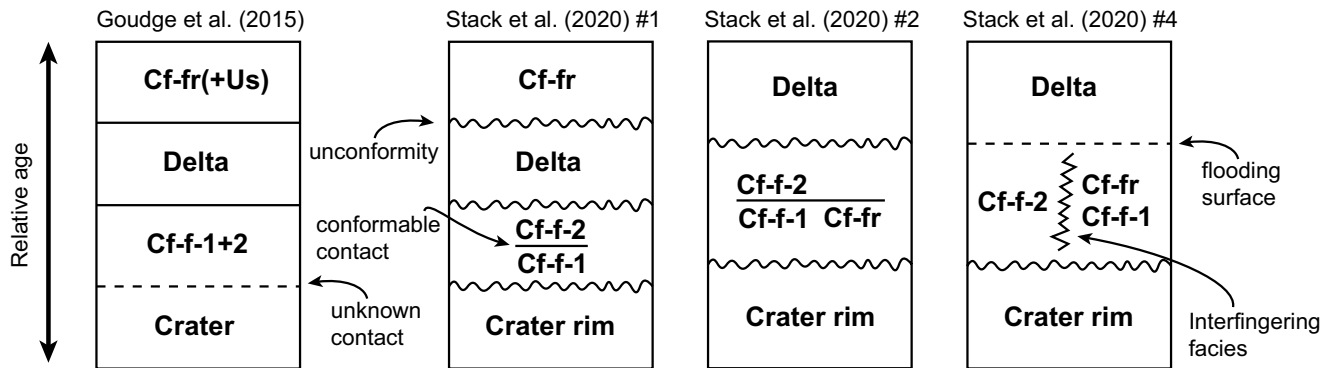


Figure 5. Hypotheses for the stratigraphic relations between geologic units in Jezero crater presented by Goudge et al. (2015) and Stack et al. (2020). Cf-fr: crater floor fractured rough unit. Us: undifferentiated smooth unit. Cf-f-1: crater floor fractured 1 unit. Cf-f-2: crater floor fractured 2 unit.

et al., 2019) and often lump these together. When discussed as a single composite unit, we refer to these units as “the youngest crater floor units.”

2.2. Western Delta Deposit

The western delta in Jezero crater has been interpreted as a river delta deposit that built out into a lake that existed in the crater (Ehlmann, Mustard, Fassett, et al., 2008; Fassett & Head, 2005; Goudge et al., 2017; Schon et al., 2012). The deposit has a fan-like plan view geometry (Fassett & Head, 2005); its surface displays pervasive layering and cross-cutting linear ridges that are interpreted as fluvial channel-belt deposits on its surface (Goudge et al., 2018). The eastern edge of the western delta deposit forms a distinct erosional scarp (Fassett & Head, 2005; Schon et al., 2012) that exposes internal layering within its walls. Schon et al. (2012) estimate that the outer third of the delta complex, specifically delta front deposition and the prodelta deposits that are potentially composed of the highest concentration of clay-size particles, have been largely removed by aeolian erosion. Lakeward of the present-day delta edge, there are also numerous isolated hills and mesas that have been interpreted as either remnants of delta deposits or isolated deposits of lacustrine strata that were deposited at the same time as primary deltaic deposition (Fassett & Head, 2005; Schon et al., 2012; Stack et al., 2020, Figure 2). Given the uncertainty associated with the genesis of these hills, they are perhaps better described as “delta-associated sedimentary deposits” to leave open the possibility that they may be lacustrine in origin rather than true delta remnants. Therefore, we will refer to these as “delta-associated remnant deposits.”

The first detailed studies of Jezero crater proposed that the dark crater floor material (Cf-fr and Us) was emplaced after deltaic activity (Goudge et al., 2015; Schon et al., 2012; Figure 5). Goudge et al. (2015) placed the Cf-fr and Us units stratigraphically higher than the delta on the basis that the units appear to embay the western delta and the northern fan in Jezero. More recently, different temporal relationships between the lithological units in Jezero have been proposed, including hypotheses that crater floor units could pre-date deltaic deposition (Ruff, 2017), or that they predate at least a portion of the delta deposits (Horgan et al., 2020; Miklusicak et al., 2020; see also Sun & Stack, 2020a). Stack et al. (2020) presented four scenarios for the stratigraphic relations of units within Jezero crater (Figure 5). One, their scenario 3, is consistent with the previously published interpretation (i.e., Goudge et al., 2015), whereas the other three—including the possibility that the Cf-fr was deposited before the delta, but the Us formed after delta deposition—require more complex depositional relations, and suggest more complex age interpretations, between the Jezero delta and other crater-fill units.

3. Data and Methods

We have studied geological features on the delta, Cf-fr, and Us units in Jezero crater on the Mars 2020 Terrain Relative Navigation HiRISE Orthorectified Image Mosaic (Ferguson, Galuszka, et al., 2020). The six HiRISE stereo pairs on this mosaic include: Jezero_E: ESP_048908_1985 and ESP_048842_1985; Jezero_N:

ESP_037818_1990 and ESP_037330_1990; Jezero_C: ESP_046060_1985 and ESP_045994_1985; Jezero_DL: PSP_003798_1985 and PSP_002387_1985; Jezero_W: ESP_042315_1985 and ESP_037396_1985; and Jezero_CR: ESP_037119_1985 and ESP_036618_1985. All HiRISE image observations reported in this study (except crater counting and fracture mapping, see below) were made on this image mosaic.

3.1. Definitions

In our stratigraphic analysis in Jezero crater, we focused on the nature of the geological contacts. We describe the absence or presence of marginal depressions, i.e., “erosional moats,” at unit contacts. Erosional moats are topographic depressions that result from differential erosion of adjacent geologic units. If higher-standing relatively less resistant material is eroded, at the contact of an embaying, or surrounding, unit with higher resistance, a moat appears as the topographically higher material is removed (see, e.g., Chapman et al., 2010; Hauber et al., 2008; Ruff, 2017). For example, if lava flows up to an island of existing, less resistant, material, a moat will appear at the unit contact as the older less resistant material is removed. Ruff (2017) pointed out the similarities between such stratigraphic contacts in Gusev crater and Jezero crater, with a focus on moats and “kipukas.” Kipukas are islands of higher-standing geologic material embayed by younger lower-standing unit(s). We are not using the word kipuka in this work, because it implies both a stratigraphic relationship between adjacent units, and a specific geologic origin (i.e., as a lava) of the embaying unit, which in this case would be the youngest crater floor unit(s).

3.2. Topographic Analysis/Profiles

The image data that we have used in this study are from the Context Camera (CTX; Malin et al., 2007) and High Resolution Imaging Science Experiment (HiRISE; McEwen et al., 2003) instruments on the Mars Reconnaissance Orbiter. Jezero crater was mapped with CTX images (5 m/px) as well as HiRISE visible image basemap (25 cm/px) and derived digital elevation models (DEMs; 1 m/px; Fergason, Galuszka, et al., 2020; Fergason, Hare, et al., 2020) acquired from web-based GIS tool CAMP (for source files for this tool, see Data availability section below; see also Calef et al., 2019; Stack et al., 2020). The data were processed in a Geographical Information System (GIS) software (QGIS (<http://qgis.osgeo.org>) and ArcMap) and cross-section profiles were constructed across unit boundaries.

3.3. Fracture Mapping

Occurrence of fractures on the Cf-fr and Us units were investigated on HiRISE images. Mapping was performed by marking fractures as polyline features in the GIS program ArcMap. A specific scale (1:3,000) was used for consistency during mapping of the fractures, which is similar to the 1:5,000 scale used during the mapping of Jezero crater by Miklusicak et al. (2020). The fractures were mapped on the area broadly recognized as the “dark-toned floor” of Goudge et al. (2015), here interpreted as the combined Cf-fr and Us. Mapped fractures represent a suite of through-going fractures, with lengths generally greater than tens to hundreds of meters (e.g., Miklusicak et al., 2020) Rather than presenting a thorough inventory of all fractures, mapping here was performed with the purpose of getting an overview of the primary orientations represented by easily visible fractures.

3.4. Crater Counting

The craters used for crater counting on three selected areas were mapped on HiRISE imagery (image IDs are 034495, area 1; 023168, area 2; 023524, area 3) in conjunction with HiRISE DEMs (McEwen et al., 2003) in ArcMap. Each crater was marked manually, using the CraterTools (Kneissl et al., 2011) plug-in to ArcMap. Using this tool, all features that could be safely determined as craters above a minimum diameter of 10 m were counted on the selected areas using three points along the crater rim to produce a circle.

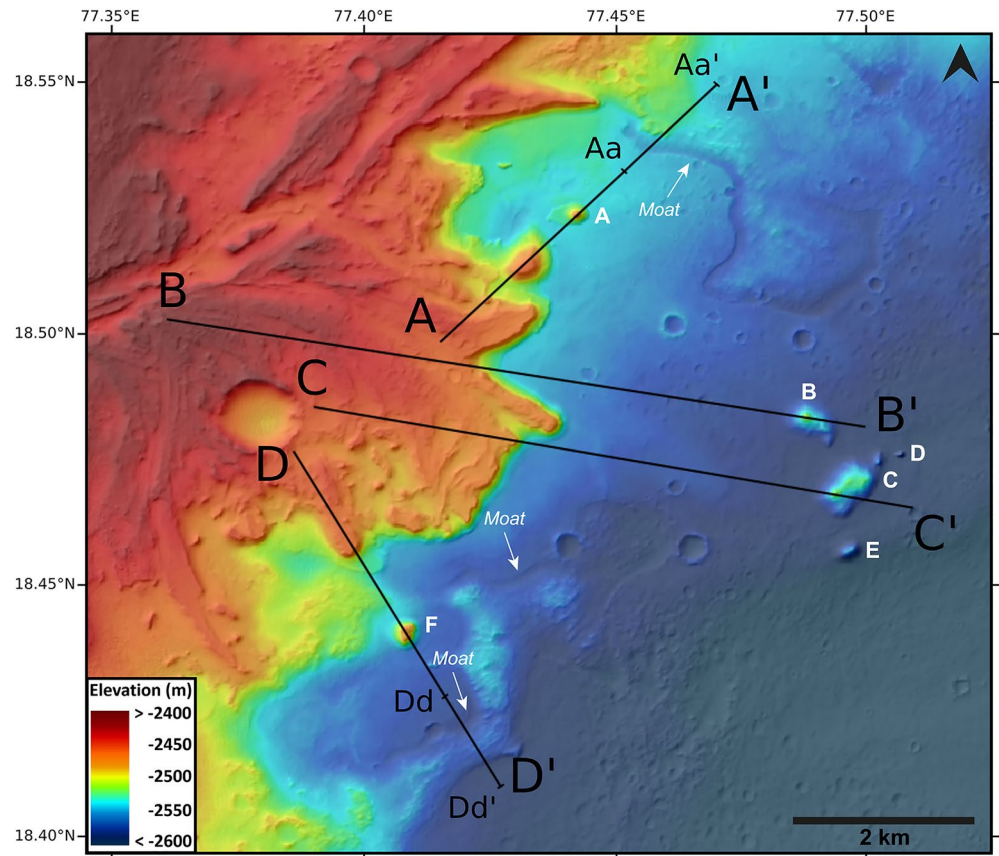


Figure 6. DEM of the study area in Jezero crater with the western delta in the left side of the image. Delta-associated remnant deposits are higher-standing features on the crater floor and five of these, labeled A-F with white bold text, are discussed in this work. Transects A-A', B-B', C-C', and D-D' represent the location of cross-sections shown in Figure 7. White arrows point to topographic depressions (“moats”) at unit contacts, as discussed in the text. For data used to produce the DEM, see Malin et al. (2007), Ferguson, Hare, et al. (2020), and the Data availability section for more information. DEM, digital elevation model.

3.5. Spectral Endmember Calculation

CRISM band parameters from Viviano-Beck et al. (2014) to isolate CRISM pixels used for spectral endmember extraction. Band parameters were calculated for image HRL000040FF using the CRISM Analysis Toolkit (CAT). We used the LCPINDEX2 parameter to illustrate the distribution of spectral signals consistent with LCP in the CRISM scene in Figure 4b.

4. Results

We analyzed the stratigraphic relations and reconstructed the sequence of events in Jezero crater by a series of investigations: based (1) on observations from profiles extending from the delta out onto the crater floor, (2) on crater counts, (3) on fracture patterns on the crater floor. For our discussion, we also use: (4) CRISM spectral data and thermal inertia and (5) comparative studies of stratigraphic relations in other craters. Our results are presented below.

4.1. DEM Analysis and Profiles

Boundaries between, and features of, units inside Jezero crater were investigated by cross-section profiles and analysis of DEMs from HiRISE scenes (Figures 6 and 7). Since the Us unit is so thin (~5 m; Golder, Miklusick, et al., 2020) elevation profiles likely reflect the topography of the Cf-fr unit, and not topographic features that are related primarily to the Us unit.

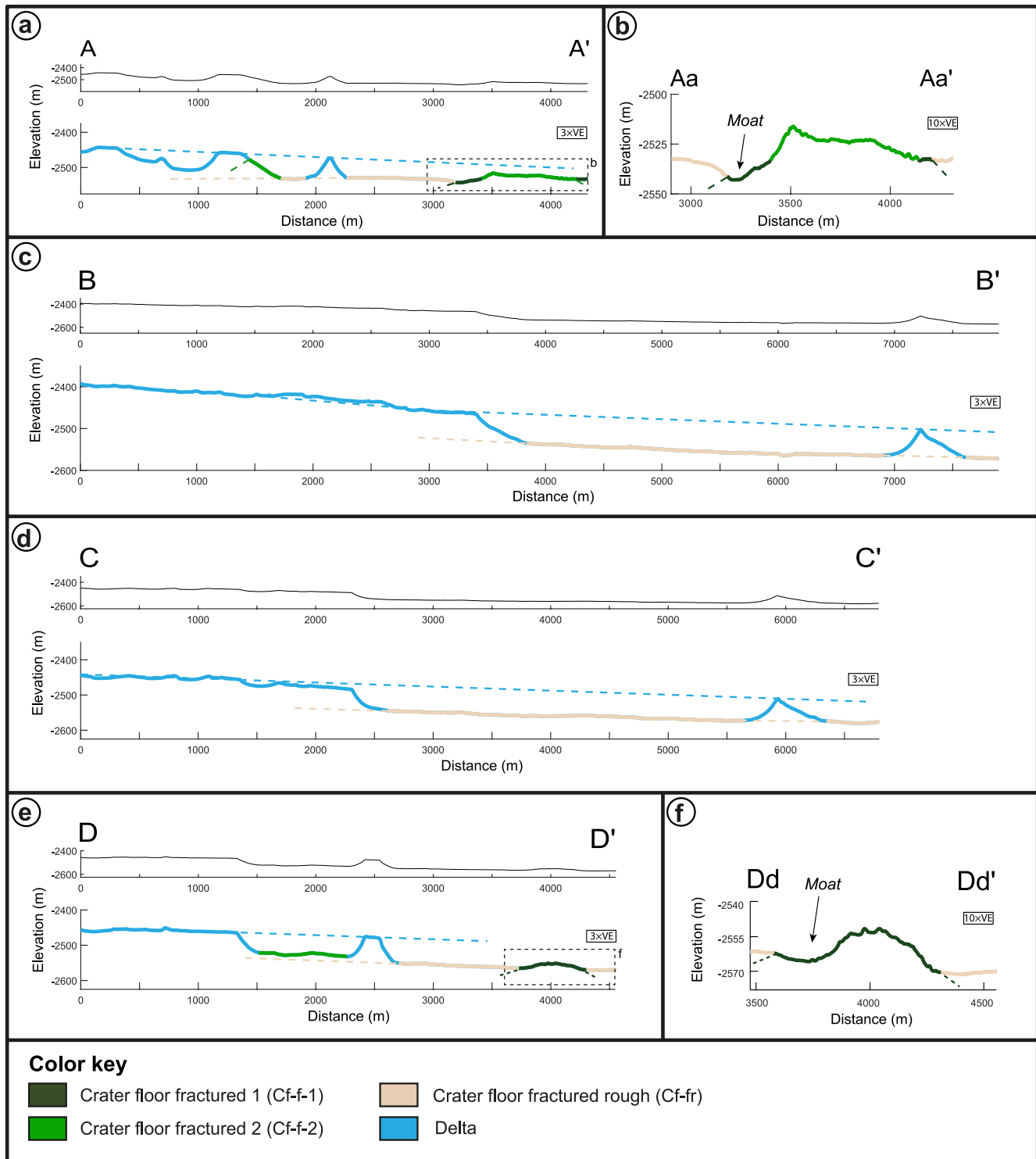


Figure 7. (a–f) Topographic profiles (see locations in Figure 6) from the western delta in Jezero out onto the crater floor. Lower version of profile at $3 \times$ vertical exaggeration (VE). Colors of the line corresponds to the individual geologic units (see key). Possible past extensions of the delta are shown as blue dashed lines, and the regional surface slope of the Cf-fr(+Us) unit is shown as beige dashed line.

The uppermost crater floor unit and the delta scarp are separated by 30–40 m in elevation, with the delta having the higher elevation. The two units are separated by sedimentary cover resulting from erosion of the steep delta scarp. The steepness of the western delta scarp immediately adjacent to the delta-crater floor boundary varies between 6° and 27°. The contact between the delta scarp and the youngest crater floor units includes both smooth and more abrupt transitions, but there is no clear evidence of a localized topographic low (i.e., a “moat”) at the contact between the delta scarp and the youngest crater floor units.

By contrast, the contact between Cf-f-1 and Cf-fr-U_s is in some places characterized by distinct narrow topographic moats (Figures 6, 7b and 7f). Such moats are more prevalent at the western side of these exposures; the eastern sides are more commonly covered by aeolian sediment, resulting from sediment transport by a prevailing easterly wind (see Day & Dorn, 2019 for discussion on wind directions in Jezero; Figure 6). Although these topographic moats are shallow (on the order of ~10 m deep; compare Figure 7a with 7b, and 7e with 7f), they form a prominent feature of these contacts (Figure 6).

Low hillocks east of the delta scarp, here referred to as “delta-associated remnant deposits,” and labeled A–F, are high-standing topographic features located on the crater floor, both close to the western delta deposit, and somewhat further to the east (Figures 6 and 8). These sedimentary deposits show a range of morphological expressions. Deposit A displays a cone-shaped cross-section profile and clear internal stratification (Figure 8a), similar to deposit F (Figure 8b). Deposits located further to the east, specifically B–D (Figures 8c–8e), also display internal stratification, but have less distinctive overall morphologies. The deposits trap bedforms along their flank slopes, obscuring the contact to the crater floor. Still, in all instances, the boundary between delta-associated remnant deposits and the adjacent Cf-fr-U_s deposits is marked by a smooth change in topographic slope on all sides. As with the edge of the main delta body, there is no clear evidence of topographic moats at the boundary between delta-associated remnant deposits and the youngest crater floor units.

Our topographic analysis also shows that the youngest crater floor units adjacent to the delta edge slope away from the delta edge, and the slope is the same as the slope of the present delta surface itself (Figures 7c and 7d). The slope is observed along axes that are radial to the delta rather than uniform across the Cf-fr-U_s units. Regionally, the crater floor preferentially slopes north to south, rather than east to west (Figure 9).

4.2. Fractures

The crater floor in Jezero is fractured at two different spatial scales (Figures 10a and 10b). Small-scale polygonal fractures are prevalent across the Cf-fr unit, and through-going linear fractures that intersect both Cf-fr and regions of the crater floor mantled by U_s materials (Stack et al., 2020). In this investigation, we focus only on these through-going linear fractures. At the mapping scale we employed, the fractures are typically between 1 and 2 m in width and range from a few hundred meter to more than 1 km in length. Fracture intersections are often orthogonal, and show both offset and cross-cutting relationships (cf. Figures 11a and 11b), which could indicate multiple fracture generations (Peacock et al., 2018). More rarely, fractures can terminate at the intersection with another fracture (Figure 11a), which may also indicate different fracture generations. Fractures also appear to intersect the ejecta and rims of craters exposed in the Cf-fr-U_s units (cf. Figure 11c). These large, linear fractures show distinct differences in their distribution across the Jezero crater floor. Most notably, large, linear fractures are recorded only within the region of the crater floor defined by the combined Cf-fr and U_s map units (Figure 10c). Fractures also appear to be more concentrated along the delta front, and appear more sparsely to the SE. This distribution, however, does not necessarily reflect a lack of fractures; fractures are more easily identifiable in regions near the delta front, which are more heavily mantled by U_s, and less easily identifiable in regions dominated by Cf-fr. Across the crater floor, there is no clear orientation for these larger, linear fractures, although fractures with the longest exposures favor a NW-SE orientation (Figure 10d; see also Miklusicak et al., 2020). In total, more than 1,700 fractures were mapped.

More detailed examination of fractures in the NE region of the Jezero crater floor, where fracturing is most dense, shows distinct patterns of fracture orientation between the edge of the western delta and the lobate margins of the Cf-fr-U_s units (Figure 10c), where fractures appear to parallel the delta scarp (Figures 10c and 10d). A similar pattern was observed by Miklusicak et al. (2020), who showed that fracture orientation

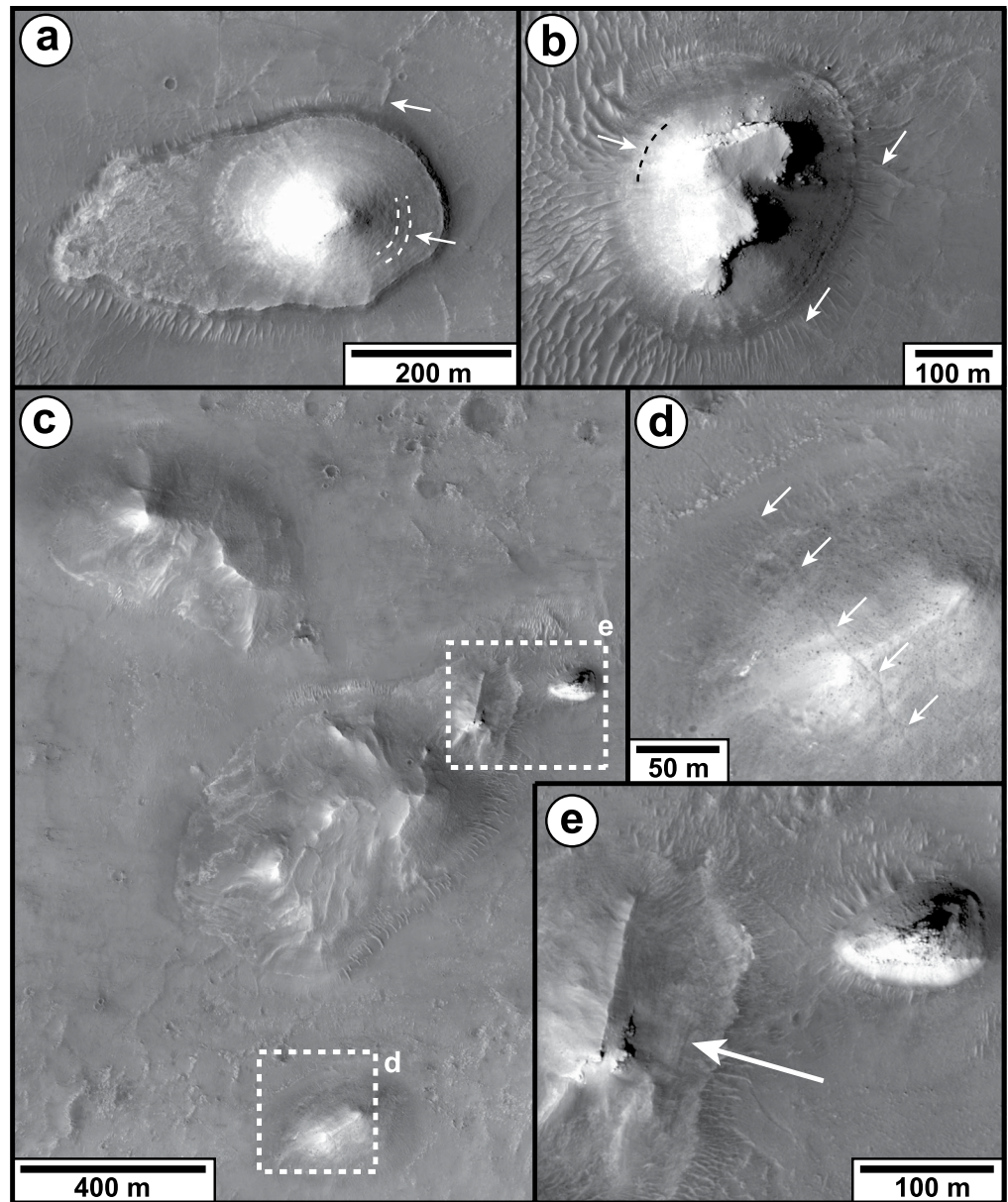


Figure 8. Photos of delta-associated remnant deposits (HiRISE image mosaic; Ferguson, Galuszka, et al., 2020). (a) Deposit A, located just east of the western delta scarp. Note prominent cone-shape. Arrows point to internal stratification and fracture that terminates at the base of the deposit. (b) Deposit F, located southeast of the western delta scarp. Arrows point to internal stratification and fractures that terminate at the base of the deposit. (c) Deposits B–E, located further east of the western delta scarp. (d) Close-up of deposit E, with arrow pointing to a fracture that crosses the deposit. (e) Internal stratification in deposit C. North is up in all images. See Figure 1c for locations. HiRISE, High Resolution Imaging Science Experiment.

shown in the southern portion of Figure 10c inset also parallel the lobate margin of the Cf-fr-U_s unit to the southeast, and are consistent with a broader pattern of fractures that occur parallel to the lobate margin of the Cf-fr-U_s unit(s). We have not observed such a relationship between fracture orientation and the delta edge further to the north, suggesting that apparent alignment of fractures to the delta front may simply reflect that the delta scarp itself in that area has the same overall shape as the lobate margin of the Cf-fr and outcrop of Cf-f-1 southeast of the delta scarp (Figures 1c and 2).

An interesting relationship also occurs between the fractured Cf-fr-U_s unit and outcroppings of the delta and delta-associated remnant deposits. First, fractures typically approach the delta front at high angles,

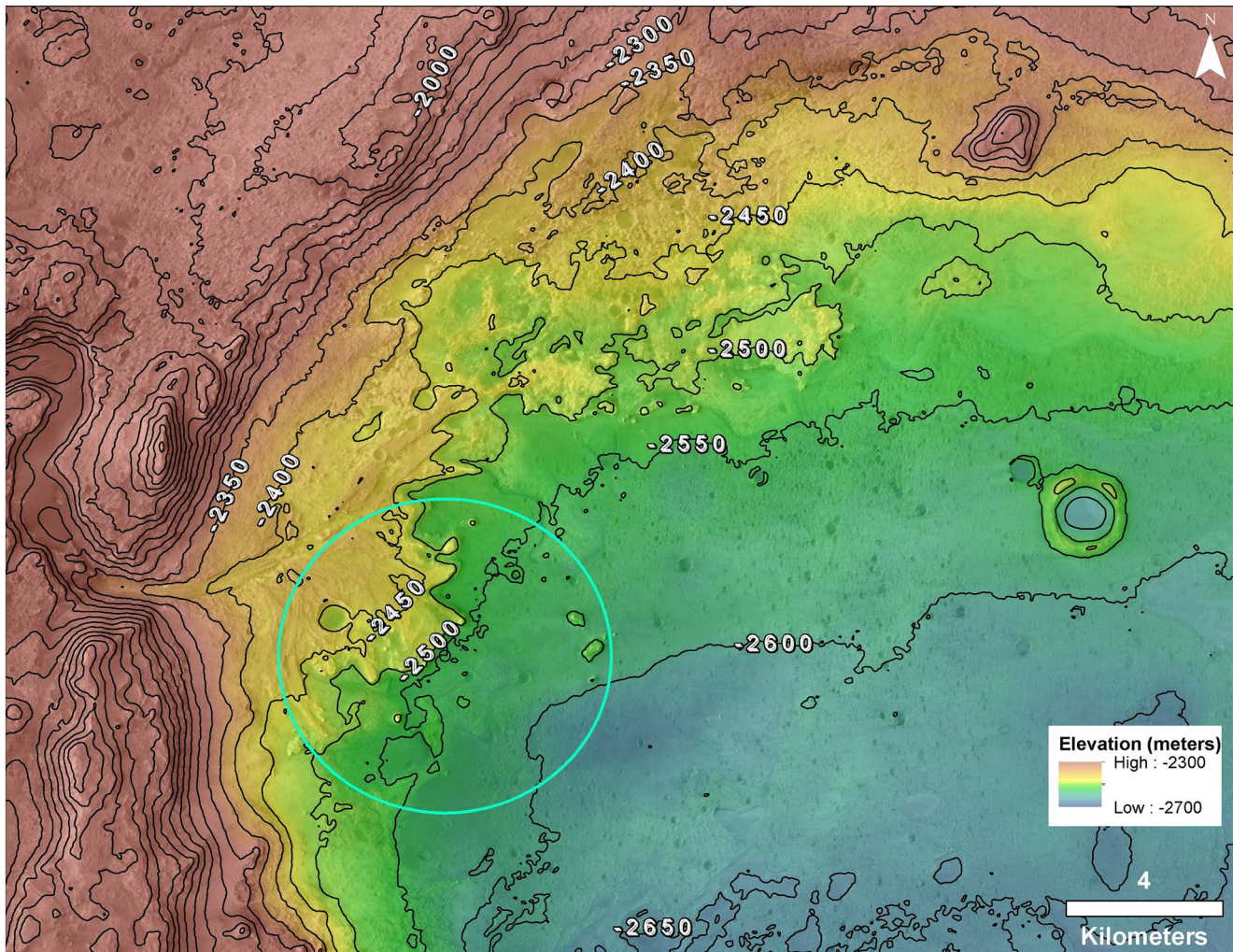


Figure 9. Topographic map of part of Jezero crater showing the slope direction of the crater floor and the landing ellipse of the Mars 2020 mission. Red lines are 50 m contours and colors correspond to topography (blue = low, green to yellow = moderate, red = high). Note that the crater floor preferentially slopes north to south, rather than east to west.

where they either terminate abruptly or are buried by sediment either eroded from the delta edge or deposited along this topographic margin as aeolian dunes (Figure 11d; see also Miklusick et al., 2020). We also observe that fractures do not cross delta-associated remnant deposits A and F (Figures 8a and 8b), but either end at the base or terminate underneath the deposit, although at least some fractures are observed to cross delta-associated remnant deposits located further to the east (Figure 8d).

4.3. Craters

The density of craters on the Cf-fr and Us units varies across the surface, which at least partially is caused by presence, or extent of, the Us unit on Cf-fr. There is a marked difference apparent to the naked eye especially near the western delta edge. All craters above a minimum diameter of 10 m were counted on three different areas, not for quantitative reasons or for establishing an age, but for displaying the differences in the number of small craters on different areas of the crater floor in Jezero (Figure 12). Craters that were counted on the three selected areas are 10–370 m in diameter, and for each area the spread in crater diameters is 10–331 m (area 1), 10–370 m (area 2), and 16–352 m (area 3). Since the area counted is limited in size (area 1: 15.35 km², 2: 8.58 km², 3: 8.19 km²), we are aware that there are limitations to our observations, but comparisons between the areas is still possible, and we hope to resolve information about the local

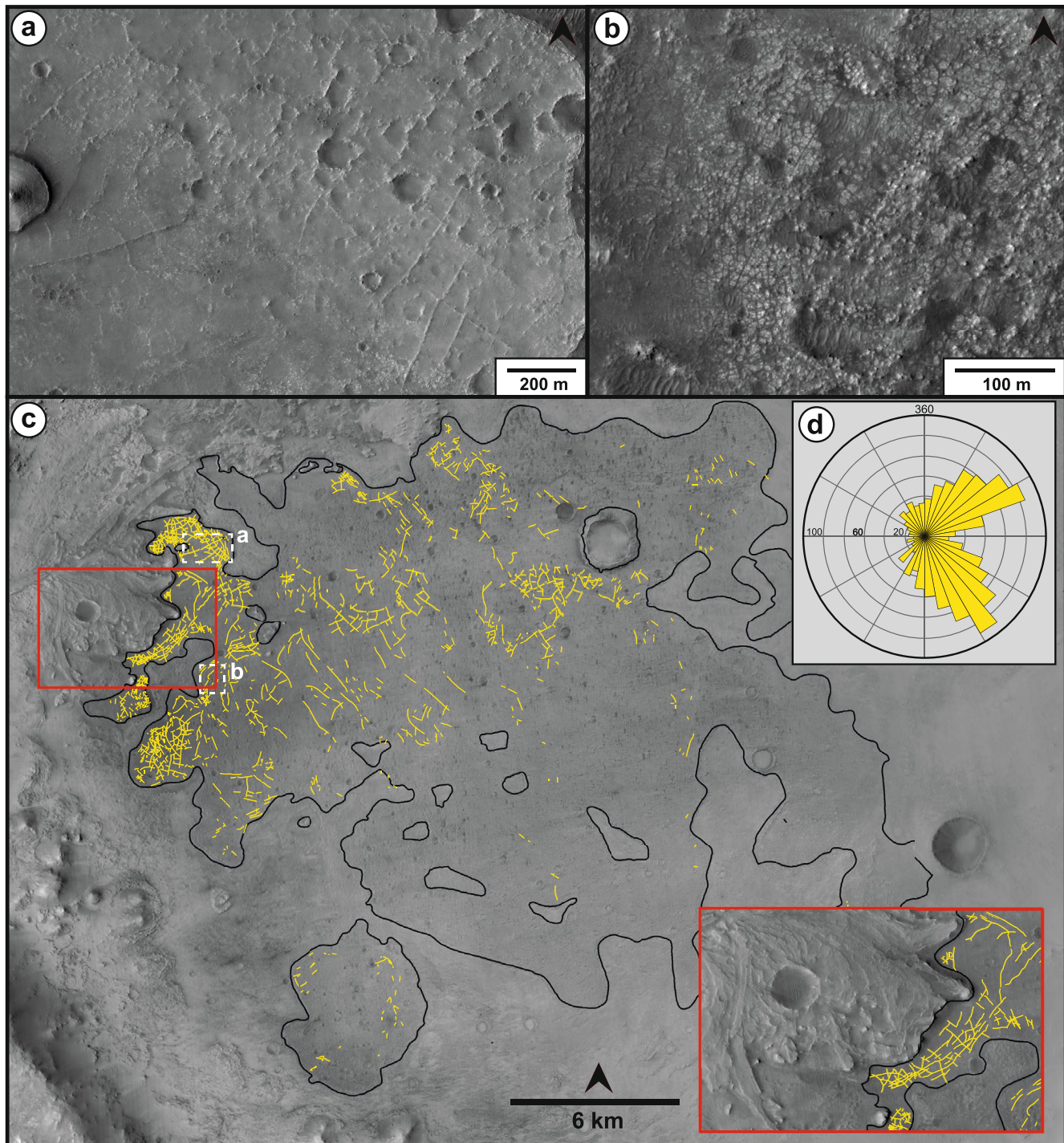


Figure 10. (a) Examples of through-going linear fractures on the Cf-fr and Us units in Jezero crater. (b) Smaller-scale polygonal fracturing characterizing the Cf-fr unit (a and b with HiRISE image mosaic as background; Ferguson, Galuszka, et al., 2020). (c) Overview of mapped through-going linear fractures (in yellow) on the Cf-fr and Us units in Jezero crater shown on CTX image. Mapped fractures are typically ~ 1 m in width and \sim a few hundred m in length. The red box in the bottom right corner is a close-up of the area where fractures have different directions than the general NW/SE direction on the unit. Black line after Goudge et al. (2015), marking the “volcanic floor unit.” (d) Rose diagram showing the trends of the all the mapped fractures from (c). HiRISE, High Resolution Imaging Science Experiment; CTX, Context Camera.

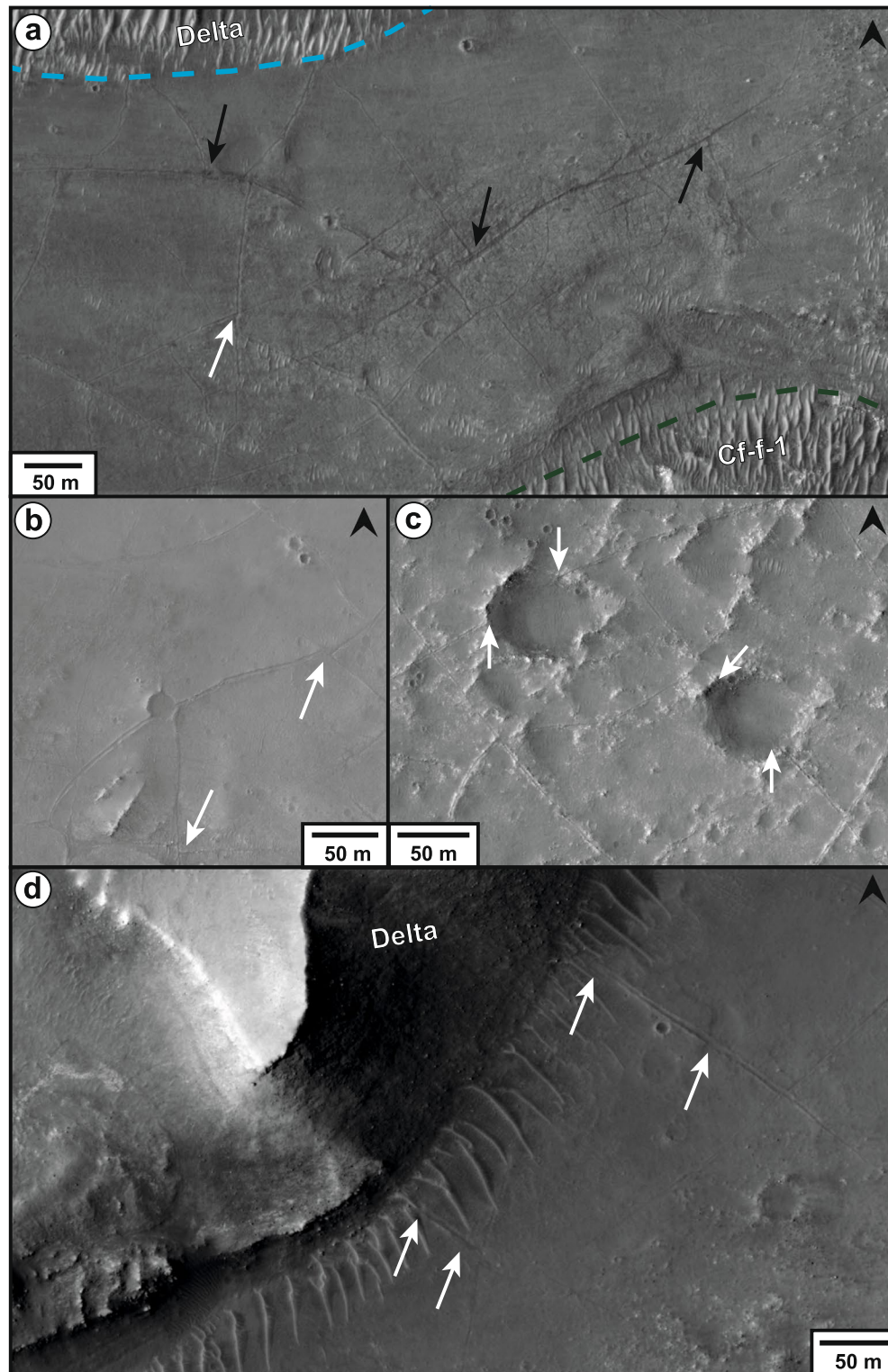


Figure 11. Fractures on the Cf-fr and Us units on HiRISE image mosaic (Ferguson, Galuszka, et al., 2020). (a) Close-up showing fractures with different general directions. White arrows point to offset relations between possible different fracture generations. Black arrows point to abutting relations between (possible) different fracture generations. (b) Close-up showing fractures that cross small impact crater on the crater floor. Arrows point to offset relations between possible different generations of fractures. (c) Fractures crossing small impact craters on the Cf-fr unit. (d) Close-up of fractures at the delta scarp. Note lack of reorientation before they disappear. See Figure 1c for location. HiRISE, High Resolution Imaging Science Experiment.

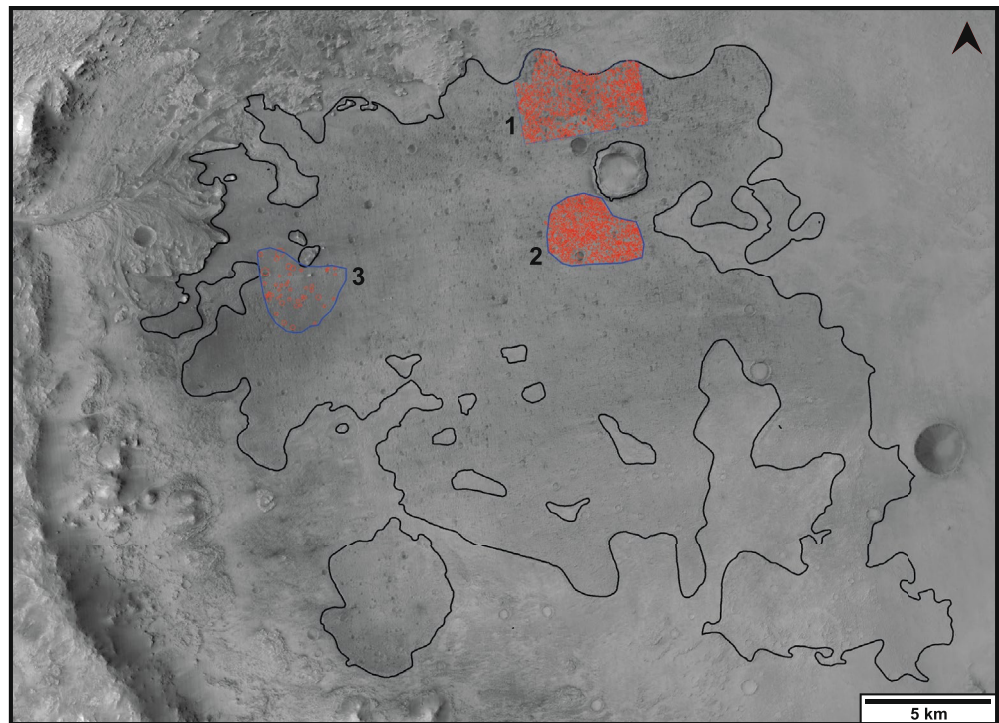


Figure 12. Close-up of the northern part of the crater floor in Jezero crater (CTX image). Areas marked with blue are areas where craters were counted. The areas are of similar size, but note the difference in number of craters counted in the area to the west compared to the two areas to the east. Total number of counted craters in area 1: 1,028, 2: 1,269, 3: 154. Black line after Goudge et al. (2015), marking the “volcanic floor unit.” CTX, Context Camera.

processes, or processes that affect only a small area [see discussion in, e.g., Kukkonen and Kostama (2018)]. Closer to the delta scarp, only 154 craters were counted (corresponding to a frequency of ~ 19 craters/km²; Figure 12), and this is where the Us unit is most prominent. On the two other areas, labeled as 1 and 2, 1,028 (~ 67 craters/km²) and 1,269 (~ 148 craters/km²) craters were counted, corresponding to a difference of a factor of ~ 8 , respectively.

Small craters, 10–20 m in diameter, on the smooth surface immediately east of the delta scarp exhibit non-rocky rims and ejecta blankets. At crater sizes of 25–30 m, rims and ejecta appear rocky (Figure 13; compare also Warner, Schuyler, et al., 2020).

5. Interpretation and Discussion

5.1. What Can Fractures on Cf-fr and Us Tell us About Stratigraphic Relations in Jezero Crater?

Several observations regarding large, linear fractures observed in the Jezero crater floor may help us interpret stratigraphic relationships. First, these fractures intersect both the combined Cf-fr + Us unit and, critically, the crater rims and ejecta that are exposed within these units (Figure 11c). These observations indicate that fracture formation is younger than both the deposition and cratering age of these floor materials. Second, on the regional scale, there appears to be no clear orientation to these large, linear fractures or any clear pattern of their intersections. These observations suggest that the origin of these fractures results from hydrofracture (i.e., the fracture of materials from the overpressuring of subsurface fluids; Gudmundsson et al., 2002; Mandl, 2005; Philipp et al., 2013). Finally, on a more local scale, observation of an apparent relationship between fracture orientation and the lobate margins of the combined Cf-fr + Us unit (Figure 10, see also Figures 2 and 6), provides critical data on the stress fields at the time of fracturing.

The pattern and orientation of fractures results from both the mechanism of fracture formation and the mechanical properties of the material being fractured (e.g., Goehring, 2013, and references therein;



Figure 13. Differences in roughness of ejecta and rim blockiness of small craters on the Us unit immediately adjacent to the western delta scarp in Jezero crater. Note blockiness of ejecta associated with the fresh crater in the center of the photo. See Figure 1c for location. HiRISE image mosaic (Fergason, Galuszka, et al., 2020). HiRISE, High Resolution Imaging Science Experiment.

Gudmundsson, 2011; Mandl, 2005). Fractures that result from tensional stresses within a single unit, such as those that occur with cooling of igneous units, desiccation of water-rich sediment, or thermal expansion and contraction tend to form discrete polygonal networks with a dominance of 120° intersection angles (Goehring, 2013; Kronyak, Kah, Miklusicak et al., 2019), and tectonic fractures are most easily recognized by a clear pattern of orientation that relates to the tectonic stress field (e.g., Gudmundsson, 2011, and references therein). By contrast, hydrofracture events most commonly lack clear orientations, except when affected by stresses associated with the boundaries of a geologic unit (Gudmundsson et al., 2002; Mandl, 2005; Philipp et al., 2013).

Observations that fractures locally appear to be oriented both parallel and perpendicular to the lobate edges of the Cf-fr + Us unit are consistent with differential stresses along the natural edge of the Cf-fr + Us unit (cf. Miklusicak et al., 2020). If this is the case, then if the Cf-fr + Us unit were younger than the Jezero delta and delta-associated remnant deposits, we would expect to see a similar fracture pattern at these margins. Such a fracture pattern, however, is not observed along the entire length of the delta front, suggesting that the fracturing process (which must occur after primary deposition of the Cf-fr unit) was unaffected by the presence of deltaic sediments. More commonly, we see fractures abruptly disappear under the bedform and talus along the boundary of the delta scarp, with no changes in fracture orientation or morphology, even when fractures can be seen traced between aeolian bedforms otherwise obscuring the contact (Figure 11d). If the western delta was already deposited at the time of the fracturing process, the weight of the sediment would be expected to create stress fields in the crater floor material leading to fracture reorientation, implying that deltaic sediments had yet to be deposited. We therefore suggest that these observations are most consistent with a scenario in which the fractures continue underneath the delta and delta-associated remnant deposits, and were simply buried during deltaic sedimentation.

Additionally, we do not observe propagation of fractures upward from the Jezero crater floor into overlying sedimentary materials of the delta and delta-associated remnant deposits. It is common for the hydrofractures to be affected by the mechanical properties of the rock units through which they propagate (Weertman, 1980). Most commonly, hydrofractures are observed to terminate at contacts where the overlying material has a strength sufficient to arrest fracture propagation (Gudmundsson & Brenner, 2001; Kronyak, Kah, Edgett, et al., 2019). The inferred fine-grained nature of sedimentary materials associated with the

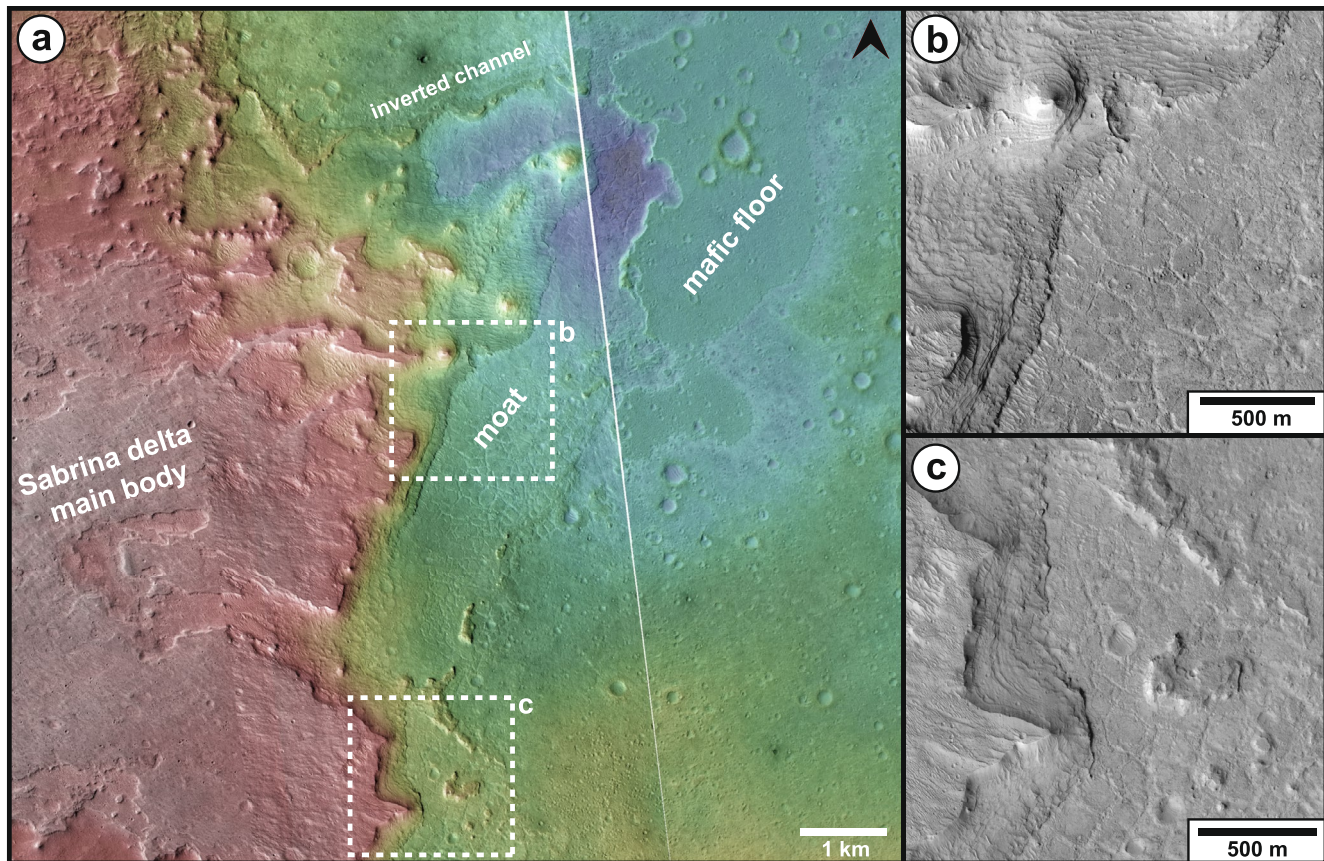


Figure 14. Magong crater, Xanthe Terra. (a) Merged HiRISE DEM showing the Sabrina Vallis fan and the mafic crater floor unit, with the moat separating the two units. (b and c) Detail of the moat showing the exposed polygonally fractured unit in the moat that forms as the fan sediments erode. HiRISE, High Resolution Imaging Science Experiment.

delta front and delta-associated remnant deposits (e.g., Goudge et al., 2017), however, and the extensive erosion of these units, suggest that the strength of these units would be insufficient to cause arrest of fracture propagation. If, on the other hand, fractures formed after deposition of the delta and delta-associated remnant deposits, the absence of visible fractures in these units would suggest that materials were sufficiently weak that pressures rapidly dissipated via formation of abundant small-scale fractures. Such fractures are not visible in orbital imaging, and our combined observations are more consistent with a scenario in which deltaic deposits are wholly younger than the fractured crater floor. The alternative scenario presented above, however, can be tested by the Perseverance rover when it reaches the delta front.

5.2. What Can We Learn From Stratigraphic Relations in Other Craters?

Investigation of the nature of, and stratigraphic relationships between, rock units in Gale crater by the Curiosity science team (e.g., Grotzinger et al., 2015; Stack et al., 2016) resulted in the recognition of a former standing body of water and an understanding that the body of water could have persisted for long enough time to have been relevant for habitability. In Magong crater, Xanthe Terra, a flat, polygonally fractured floor has been exposed where active erosion of the Sabrina Vallis fan results in a moat between the fan and the crater floor unit (Knade et al., 2017, Figure 14). This moat marks the eroded margin of the fan, at least along the entire southern and eastern sides (Knade et al., 2017) and it is interpreted that the dark-toned, mafic crater floor unit is both younger than the fan and more erosionally resistant than the fan. These observations thus allow constraints of stratigraphic relationships between fan and crater floor units in Magong crater. We do not observe moats between the delta and youngest crater floor units in Jezero crater, either where the delta is eroding away, exposing the underlying units, at the western delta scarp, or in association with

delta-associated remnant deposits (Figure 7). The Cf-fr and Us units consistently continue all the way up to the sediment cover at the base of the western delta scarp, with no underlying unit exposed in between, either because it is not present or is covered by sediments (see, e.g., Figures 8a and 8b). If such a moat is present but obscured by talus and aeolian sediments, it is clear that there was very limited scarp retreat since emplacement of the youngest crater floor unit (compare the exposed moat in Magong crater; Figure 14). The youngest crater floor unit(s) either formed $\sim 2\text{--}2.5$ Ga, or has been exposed since that time (Shahzad et al., 2019; Warner, Schuyler, et al., 2020), and insignificant scarp retreat since then is not consistent with erosion rate estimates (e.g., Golombek & Bridges, 2000; Golombek et al., 2006; Ramirez et al., 2020), especially of nonresistant deltaic material which is known to erode relatively fast given the lack of small craters on the delta (Mangold et al., 2020). Moats at contacts between a young resistant unit overlying an older less resistant unit in Gusev crater can be compared with features in Jezero (Ruff, 2017). Ruff (2017) noted the presence of moats between kipukas and the crater floor lava flows in Gusev, and that such moats were also present in Jezero, but only at contacts between the Cf-f unit and the Cf-fr/Us. Ruff (2017) suggested that one explanation for the lack of moats at delta-associated remnant deposits can be explained by the hypothesis that the delta is older than the floor if the rate of erosion of the embaying Cf-fr+Us unit keeps pace with or outpaces that of the delta-associated remnant deposit material, which is inconsistent with observations of crater retention between the units, and that the Cf-f erodes more easily than the delta-associated remnant deposits. However, the lack of moats around the western delta and delta-associated remnant deposits in Jezero (Figure 7) is also consistent with the current expression of the delta being younger than the floor and overlying the floor units, something that was also noted by Ruff (2017). As a comparison, moats can be easily observed around the western margins of the Cf-f-1 unit in a map showing elevation relationships in Jezero (Figure 6). There are no western margins between the main western delta body and the crater floor units, but moats are lacking on all sides of the delta-associated remnant deposits.

Combined, the absence of an erosional moat and inferences based on fracture orientation are consistent with a scenario in which at least some sedimentary rocks of the delta deposit postdate deposition (and potentially fracturing) of the youngest crater floor units.

5.3. Constraining the Relative Timing of Events in Jezero

The relative age of the western delta in Jezero has been estimated by buffered crater counting of river valleys (Fassett & Head, 2008a) and by crater counts on the delta itself (Mangold et al., 2020), but can be further constrained by the inferred relation between deltaic sediments and the crater floor unit. Fassett and Head (2008a) concluded based on buffered crater counts of inlet valleys, that fluvial activity ceased about 3.8 Ga, and Mangold et al. (2020) presented an age of the delta itself of 3.2–3.6 Ga based on crater counting. These crater count ages would seem to argue that the delta predates emplacement of the youngest crater floor unit (Cf-fr and Us), although the 3.2–3.6 Ga age for the delta is close to the age of the floor, if the full age within error is considered [2.6 ± 0.5 Ga; Shahzad et al., 2019; see also discussion in Marchi (2021)]. Dating small surface areas such as the Jezero western delta using crater counts involves significant uncertainty (Palucis et al., 2020; Warner et al., 2015; see also Quantin-Nataf et al., 2019).

A late-stage reactivation of the proximal section of the fluvial system feeding sediment into Jezero has been proposed from differences in valley morphology (Mangold et al., 2020). Reactivation of the valley's lower sections could lead to renewed progradation of the delta and sediment accumulation on the delta surface, without significantly affecting the buffered crater counts on the valley system as also argued by Mangold et al. (2020). Many craters on the delta surface are formed onto the youngest ridge-formed deposits inferred to be former river channel-belt fill, and thus postdate the last phase of fluvial activity, but there are some examples of craters on the delta that show possible evidence of modification by fluvial activity and thus may predate some fluvial activity (Figure 15). We note, e.g., that there are channels that appear to cross craters (Figure 15c), though more robust analysis is needed. Horgan et al. (2020) stated that the state of preservation of the western delta deposit—by comparison to the northern crater-edge sedimentary package (northern fan)—could potentially be explained by the uppermost exposures being significantly younger than stratigraphically lower deposits, or that they could be potentially older delta deposits preserved in the northern part of the crater. This is consistent with the understanding that sporadic fluvial activity on Mars potentially extended into the Hesperian/Amazonian (e.g., Goddard et al., 2014; Grotzinger et al., 2013, 2015; Hauber

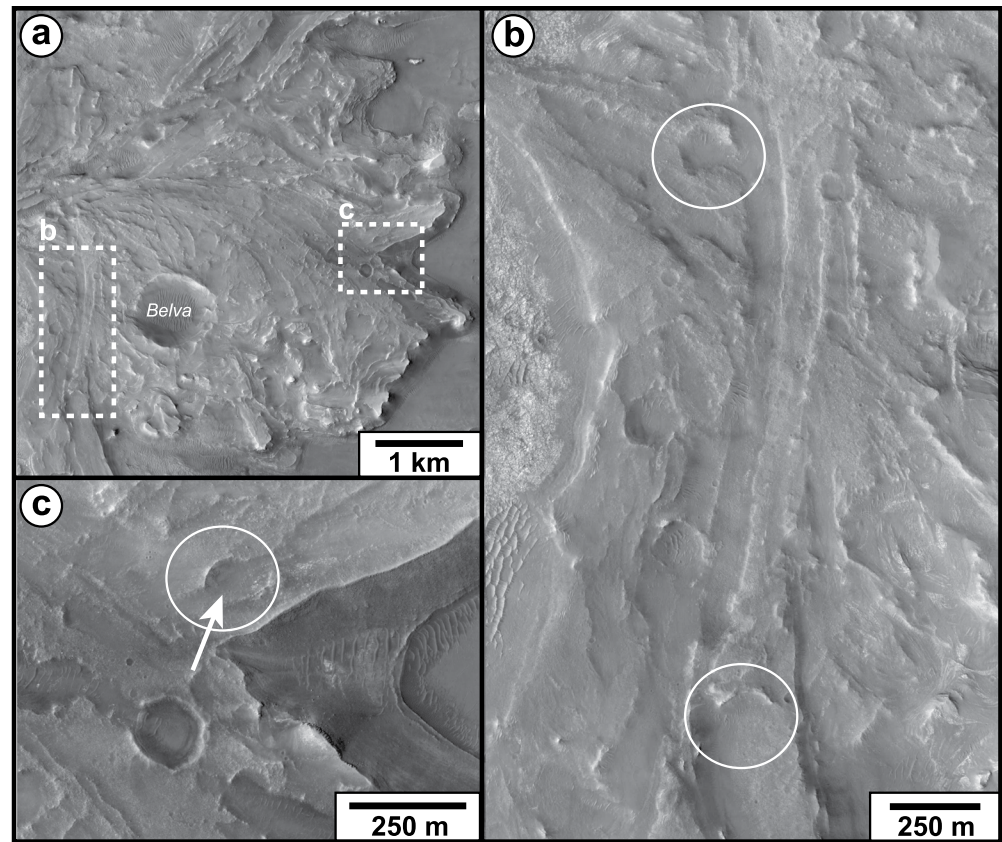


Figure 15. Craters on the western delta in Jezero. (a) Overview image of part of the delta. Note the large crater, Belva, with a relatively well-preserved rim. (b) Examples of craters that potentially could predate a phase of fluvial activity on the delta (marked with circles). (c) Crater with channel (?) crossing through. The arrow points to a ridge that marks a potential channel. HiRISE image mosaic base (Ferguson, Galuszka, et al., 2020). HiRISE, High Resolution Imaging Science Experiment.

et al., 2013; Kite et al., 2019; Salese, Di Achille, et al., 2016; see also discussion below). A scenario of multiple episodes of deposition forming the western delta needs validation from observations on the surface in Jezero, or could even require sample return. Nevertheless, we want to highlight here that discharge fluctuations leading to intermittency is likely a relevant factor if the delta developed over an extended period of time, as opposed to Jezero lake formation due to a catastrophic event (see discussion in, Salese, Kleinhans, et al., 2020). Such a scenario may also be consistent with distinct differences in the dominant primary mineralogy observed in different delta facies, which could suggest major changes in the watershed geology over extended periods of time (Horgan et al., 2020).

The derived age of the floor can also be questioned. It is possible that the Cf-fr unit was covered at some point, and has been gradually exposed for an extended period of time (Quantin-Nataf et al., 2021; Warner, Schuyler, et al., 2020). This would mean that an overlying protective unit(s) has prevented new craters from forming on the Cf-fr unit and that the derived model age therefore represents an “exposure age” of the surface rather than continuous crater accumulation since the original deposition of the unit. The crater data (Shahrzad et al., 2019; Warner, Schuyler, et al., 2020) indicate that the Cf-fr unit must have been mostly exhumed and exposed to erosion by 2.0–2.5 Ga to explain the crater counts. Erosion of the unit is still ongoing, explaining the abundance pattern of small craters observed by Warner, Schuyler, et al. (2020). If the Cf-fr unit was in fact covered and has been exhumed, this leads to important constraints for Mars sample return concerning potentially using this unit for tying the Martian crater chronology to an absolute age [e.g., Herd et al., 2021, see also discussion in Shahrzad et al. (2019)].

In summary, we cannot rule out a scenario where the delta postdates emplacement of the Cf-fr-U_s units based on the crater counts on the delta, or on the floor. We find that it is possible that the delta developed over a protracted time period, with potentially several reactivation episodes. The last stage could have been very much later (on the order of 0.5–1 Ga) than when delta deposition first started, based on the late-stage reactivation scenario presented by Mangold et al. (2020) and significant differences in preservation state between the western delta and northern fan in the crater.

In the stratigraphic scenario proposed here (Figure 16), the original morphology of the Jezero impact crater is obscured by crater-fill deposits. The youngest of these deposits are Cf-f-1 and Cf-f-2. These crater-fill deposits were exposed at the surface long enough to become both cratered and eroded, forming relief along the crater floor. The origin of Cf-fr is ambiguous, but the exact origin does not have an effect on the broad temporal scenario proposed here. For example, Cf-fr could represent an extrusive volcanic deposit formed during a paused episode of fluvial activity in Jezero, or an additional episode of fluvial or aeolian sedimentary emplacement, erosion, and cratering, wherein Cf-fr is more resistant to erosion than Cf-f-1 and 2, resulting in the formation of moats (e.g., Figures 7a, 7b, 7e and 7f). An alternative scenario has been proposed by Kah et al. (2020) wherein Cf-fr represents the eroded upper surface of Cf-f-1 and Cf-f-2 that has been made more resistant to erosion by the association with the U_s unit. However, this hypothesis may not be consistent with the spectral properties of the units as Cf-f exhibit strong olivine signatures, which are rare in both Cf-fr and U_s (Horgan et al., 2020).

Regardless, in our scenario, the western delta is deposited on top of at least the Cf-fr unit (possibly along with the U_s unit), which in turn is followed by erosion of all units, including delta deposits, and formation of delta-associated remnant deposits that can be observed today. We leave open the possibility that the western delta may have formed through an extended series of depositional events, some predating Cf-fr and some postdating Cf-fr, that event including the formation of the current expression of the delta, until there is further understanding of the relationship between fractures and the delta edge. In either case, the Cf-fr (and possibly U_s) units were emplaced during a phase of ongoing (for fluvial sediments) or temporarily paused (for aeolian sediments) lacustrine/fluvial activity. This scenario is similar to scenarios 2 and 4 described in Stack et al. (2020; Figure 5), and thus also similar to scenarios proposed by, e.g., Ruff (2017), Horgan et al. (2020), and Miklusicak et al. (2020), although we have reinforced the “younger deltaic deposition-scenario” by investigation of stratigraphic relationships. Our scenario thus explains the relatively well-preserved state of the western delta, the unit contacts observed between crater floor units and crater floor units and delta deposits, and the varied surface texture of the crater floor in terms of smoothness. Contradicting surface ages resulting from crater counting could potentially result from capping of the Cf-fr unit preventing new craters from forming, although we have highlighted the significant uncertainty associated with derived ages both of the Cf-fr unit and of the delta. Our scenario is also consistent with the idea that Martian geological history is characterized by complex cycles of erosion of and deposition in fluvial/lacustrine environments, with significant periods of hiatus (e.g., Edgett et al., 2018; Kite, 2019; Kite et al., 2017, 2019; Malin & Edgett, 2001; Salese, Ansan, et al., 2016).

It is possible that the delta-associated remnant deposits A–F were deposited in deeper water, profundal lake environments, even though they are tied to the same depositional system. Deposits B–E (located further east of the western delta scarp; Figure 8) have somewhat different morphology than deposits A and F. They have a more hummocky expression, in fact similar to the surface expression of the northern delta in Jezero. Fractures can also be observed to cross delta-associated remnant deposits in this area further east of the western delta scarp (Figure 8d), whereas fractures terminate at the base of deposits A and F and the western delta (Figures 8a, 8b and 11d). This could be consistent with different timing of formation, possibly because they represent basin fill deposits (i.e., profundal lake deposits) rather than “true” delta remnants. Different timing, and mechanisms, of formation could also mean that the sedimentary rocks constituting these deposits have different mechanical properties that lead to differences in tendency to fracture, causing the observations that we have made. Given that these deposits are located further to the east, they are also likely to have experienced increased weathering and erosion as well, which likely caused variations in morphological expression compared to deposits closer to the delta scarp.

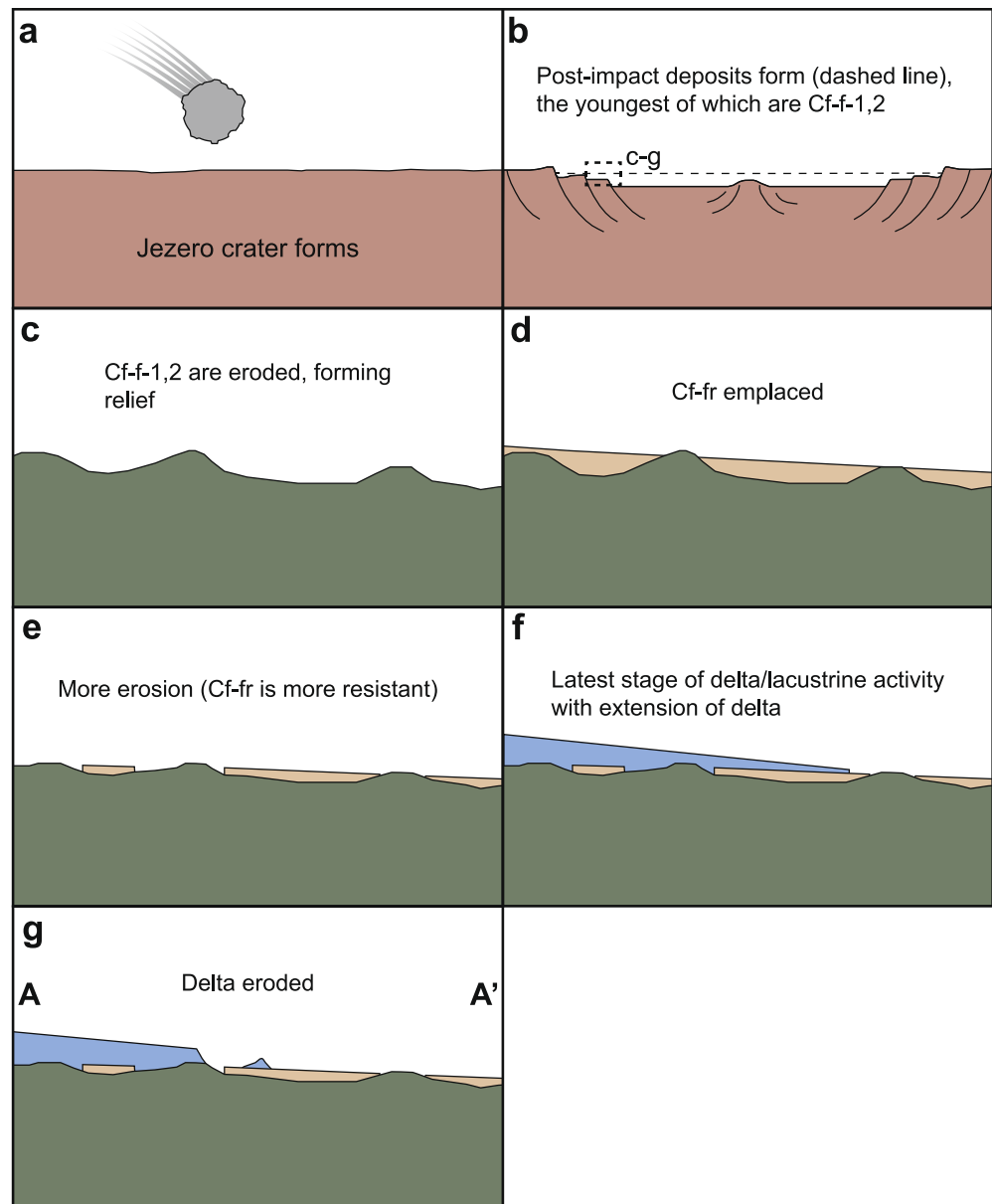


Figure 16. Overview sketch of our scenario for a sequence of events in Jezero crater. The profile shown in c–g is roughly along our A–A' profile (Figure 7). Note that this figure does not take into account potential cover and later exhumation of the Cf-fr unit, but is focused at showing the relation between the delta and Cf-fr. (a) Jezero crater forms in the Noachian period (see main text). (b) The crater is eroded and postimpact deposits form, covering the central uplift of the structure [modified after Osinski et al. (2018)]. The youngest crater-fill deposits at this stage are Cf-f-1 and 2. (c) Cf-f-1 and 2 are eroded, forming relief. (d) The crater floor fractured rough (Cf-fr) unit is emplaced. (e) Cf-fr and Cf-f-1,2 are eroded, and between the three units, Cf-fr is the more resistant unit, leading to formation of topographic depressions, moats, at the contacts between Cf-fr and Cf-f-1,2. (f) At the latest stage of fluvial/lacustrine activity in the crater, the western delta extends out into the crater. (g) More erosion, including of the delta. This results in the formation of delta remnants.

Elevation profiles presented here show that the delta and the delta-associated remnant deposits line up, so we have used the deposits to estimate the potential past extent of the delta (Figure 7). The past extent of the delta coincides with the prominent smoothness of the floor (i.e., the mapped extent of the Us surficial cover.

5.4. Genesis of the Cf-fr and Us Crater Floor Units

As stated above, the youngest crater floor units in Jezero crater have previously been grouped together, and attributed to volcanism (preferably flow-related emplacement resulting in lobate margins; e.g., Goudge et al., 2015; Ruff, 2017). In some more recent studies (e.g., Golder, Miklusicak, et al., 2020; Stack et al., 2020; Sun & Stack, 2020b) other formational histories for the units were suggested. Edgett et al. (2018) pointed out that crater-retaining sedimentary rock units on Mars can be confused with lava plains. Some important observations on differences in lithological aspects of the units investigated here can be made from the ability to retain craters [see discussion in, e.g., Warner, Grant, et al., 2020]. The delta materials are sedimentary, and small craters do not preserve well on the delta (Mangold et al., 2020) compared to the Cf-fr unit (Warner, Schuyler, et al., 2020).

HCP in the youngest crater floor unit(s) (Horgan et al., 2020) distinguishes them from the other units in Jezero crater, including the delta deposits. In fact, HCP-composition is associated with more evolved magma compositions of Hesperian and Amazonian volcanics (Mangold et al., 2010; Mustard et al., 2005). While HCP is unique to the Cf-fr in Jezero, it is observed as the main spectral signature of a regionally extensive thin mantling unit, “the pitted capping unit,” outside of Jezero crater (Goudge et al., 2015). Thus, this similarity could either suggest a shared origin for the youngest crater floor units and the regional mantling deposit, or that the HCP-bearing materials are sourced from aeolian reworking of these regional units (Horgan et al., 2020). Alternatively, in a similar scenario, the HCP-bearing materials could be sourced from fluvial reworking of those regional units.

Our topographic profiles (Figure 7) show that the Cf-fr unit has a slope equivalent to that of the upper surface of the western delta. The inclination is along axes that are radial to the delta rather than uniform across the unit. This slope toward the crater center may represent a primary paleo-depositional inclination of sediments laid down on the lake floor of the ancient delta-lacustrine sedimentary system, which would have deepened to the east. The inclination direction that we observe is different from the general slope of the crater floor in Jezero, which is preferentially from north to south rather than from east to west (Figure 9). This is suggestive of a common origin of the Cf-fr and delta, although processes resulting in emplacement of a material mantling existing topography, such as a volcanic deposit, could also be consistent with the observation. Topography-mantling erupted material is typically thin tephra fall deposits or ash turbidites on Earth, although mass flows that thicken into depressions and areally limited, valley-confined lava flows can modify topography without forming all new relief (Manville et al., 2009). If the Cf-fr was emplaced as a regionally extensive lava flow this observation is more difficult to explain, unless there has been significant tectonic activity tilting the area postdeposition. To our knowledge, no such large-scale regional activity that could cause such tilting has been discussed. Also, large-scale regional tectonic activity causing tilting as observed by us would be expected to manifest itself as consistent tilt in one direction, rather than tilt radial to the delta. Aside from these primary formation mechanisms there is also the possibility that differential weathering and/or erosion has influenced the topography of the landscape, creating the observed regional slope.

Small craters are significantly less common on the areas that have more prominent mantling of the Us unit (Figure 12), and these areas are preferentially located just east of the western delta edge. The material that constitutes the Us has clear and distinct HCP signatures away from the delta, but near the delta edge the signature is a mix of HCP and LCP (Figures 4a and 4b; see also Horgan et al., 2020), meaning that the Us is delta-like in CRISM-signature close to the delta scarp. There is no HCP anywhere else in the crater, meaning that it is not likely that the material has an external source and was recently deposited as, e.g., aeolian sediment. Given that the material has a spectral signature that is different than the delta itself (Horgan et al., 2020), an origin as wind-blown material that exclusively originates from the delta is unlikely. This is also inconsistent with predominant wind directions in Jezero, which are east to west (Day & Dorn, 2019). The observations are suggestive of a scenario where the Us is an in-place unit (e.g., consistent with the hypothesis of Warner, Schuyler, et al. (2020) where the unit is interpreted as regolith), although it could be

locally deflated. The HCP signal could be sourced from the primary mineral composition of the Cf-fr unit. The unit is unlikely to be sourced from deflation of the Cf-f units because deflation of this surface produces sediments with strong olivine signatures (Horgan et al., 2020), so it must be a distinct unit. Given the distribution of pixels with absorptions consistent with more LCP-rich material, which are concentrated near the western delta front and also around the delta-associated remnant deposits, it is likely that variations in LCP modal abundance are changing the CRISM absorptions, with LCP-rich material derived from or preserved by the eroding delta having higher abundance near the deltaic material. The LCP/HCP signatures of the broader crater floor region (Horgan et al., 2020) correspond to a clearly arcuate region of low thermal inertia (Figure 4c) that appears to possibly correspond with Us and, based on the arcuate shape, to the past extent of the youngest delta deposits. The nonblocky nature of rims and ejecta of small craters formed onto the Us just off the delta scarp (Figure 13) is constant with the thermal inertia observation of the Us unit.

We find that erosion of the delta scarp could expose the Us unit which is stratigraphically higher than the Cf-fr unit, or alternatively that the units are genetically related and that erosion of the delta edge leaves the Us behind. Given the decreased mantling of craters toward the east by the Us (Kah et al., 2020), it is possible that the Us has had a previously more extensive distribution but has eroded to expose the Cf-fr unit. A surface exposed on Mars for 2.5 Gyr (i.e., the age of the “dark-toned floor unit” in Jezero (Shahrazad et al., 2019), should have a significant regolith cover (e.g., Hartmann et al., 2001; Warner, Grant, et al., 2020), unless surface processes have removed the regolith or the surface was protected [e.g., covered; see discussion in Rogers et al. (2018)]. Regardless of whether the hypothesis of Warner, Schuyler, et al. (2020), that Us is that regolith, is correct or not, regolith is very thin or largely missing on the Cf-fr unit in the investigated area, except for just off the delta scarp. This indicates that Cf-fr (and Us?) was either buried and later exhumed (preventing a regolith from forming; see Quantin-Nataf et al., 2021) or that the unit has been stripped of its regolith (see Warner, Schuyler, et al., 2020). These scenarios are both also consistent with observations of crater distribution, as pointed out by us, with significant difference in crater density close to the delta and also discussed by Warner, Schuyler, et al. (2020). A relation between the Us unit and the delta (or alternatively former cover by the delta) is strengthened by the clear association with the thickness of the smooth unit increasing with proximity to delta, and the fact that undifferentiated smooth material also occurs on/in the delta (Stack et al., 2020). A possible scenario is that Us could be formed by deposition of relatively larger-sized particles after reactivations of the fluvial system after periods of dormancy [see discussion in Mangold et al. (2020)]. In fact, the proximal part of the inlet channel has a spectral signature consistent with presence of HCP (Horgan et al., 2020).

5.5. Implications for the Aqueous History of Jezero

Fluvial activity on Mars did not end with the demise of the late Noachian fluvial stage. In addition to large outflow channels (Head, 2007, and references therein), evidence for at least episodic fluvial activity has also been presented, e.g., in the form of reactivation of Noachian valleys (Baker & Partridge, 1986), impact-induced melting of ice (Morgan & Head, 2009), morphology of alluvial fans (Goddard et al., 2014; Kite et al., 2017) and deltas around Chryse Planitia and the Aeolis region (Hauber et al., 2013), fluvial landforms on fresh impact ejecta (Mangold, 2012), and estimations of runoff production over time (Kite et al., 2019), as well as evidence for lacustrine activity in Gale crater extending into the Hesperian era (e.g., Grotzinger et al., 2013, 2015). Late-stage reactivation of the downstream part of the fluvial system feeding sediment into Jezero crater has also been proposed by Mangold et al. (2020). In the near-Jezero region, there is considerable evidence for fluvial activity extending well into the Hesperian illustrated, for instance, by the presence of an alluvial fan inside of Hargraves crater (which is Hesperian in age; Goudge et al., 2015; Mangold et al., 2007), and observations of fluvial landforms in the Syrtis Major area [Mangold et al., 2008; see also discussion in Mangold et al. (2020)]. We suggest that at least one episode of fluvial reactivation happened after deposition of the youngest lithified crater floor unit, here taken as the Cf-fr unit, because we show that the youngest deltaic sediments clearly occur higher in the overall stratigraphy than the floor units.

As discussed, the ages obtained from crater counting on the floor and western delta are not necessarily straight-forward to transfer to an estimate of the timing of fluvial activity in Jezero. Therefore, we are limited to reporting that there was fluvial activity in the area after deposition of the youngest crater floor units. Further support for late-stage fluvial deposition, even if short-lived and limited in terms of sediment

volume delivery to the lake, is the general slope of the crater floor, which is more prominent from north to south than from west to east (Figure 9). One possible explanation for this observation is that deposition from the north had a greater impact on the crater floor geomorphology than deposition from the west that resulted in the current expression of the western delta. Temporary late-stage fluvial activity on Mars has been attributed to numerous processes, such as climate variations (Kite et al., 2017, 2019), volcanic activity (Gulick, 1998; Gulick & Baker, 1990), and impact cratering (Goddard et al., 2014; Mangold, 2012; Salese, Di Achille, et al., 2016; Segura et al., 2008), although the process inducing late fluvial activity in Jezero crater specifically, is not presently known (Mangold et al., 2020). Given that late-stage reactivation of the fluvial system might not have happened during a time of more broadly habitable conditions, but rather during a short-lived temporary humid episode (see references above), our observations are relevant for searching for signs of past life in Jezero crater. Our observations also improve the understanding of crater floor materials and their stratigraphy in Jezero, something that is essential for sample collection strategies (e.g., Farley et al., 2020).

We have presented hypotheses for the stratigraphic relations between and origin of units in Jezero crater that ultimately will require in-situ investigation, or even sample return, for testing. Analysis of high-resolution images, geochemical and spectral data, and ground-penetrating radar data acquired by instruments on Perseverance will provide critical insights into the complex geologic history of Jezero crater.

6. Conclusions

We present new observations of the stratigraphic relationship between crater-fill units in and near the landing area for the Mars 2020 mission in Jezero crater. Analysis of topographic profiles and DEMs across the western delta and crater floor units reveal that the present expression of the delta, i.e., the present delta scarp and delta-associated remnant deposits, is younger than at least the youngest significant crater floor unit (Cf-fr), and possibly also the thin mantling unit that is on top of it (Us). We present the following observations in support of that hypothesis:

1. The boundary between the Cf-fr and Cf-f-1 units is characterized by shallow depressions, or “moats.” Moats are lacking between delta scarp/associated remnant deposits and the Cf-fr unit. At the contact between the youngest crater floor units and delta-associated remnant deposits, the floor goes right up to the deposits without exposing another unit.
2. In addition, we find the youngest crater floor unit(s) slope away from the delta, and this inclination is along axes that are radial to the delta rather than uniform across the unit. This may be consistent with a shared origin, although, e.g., an overlying mantling unit draping existing topography cannot be excluded.
3. Fractures on the youngest crater floor units that are oriented roughly perpendicular to the delta scarp abruptly end at the scarp, and we find that one possible explanation for this observation is that the fracture-forming event took place before the western delta was deposited.
4. Small craters are sparse on areas of the crater floor where the Us unit is most prominent (proximal to the delta), indicating recent coverage of the Cf-fr unit close to the delta by some overlying unit.
5. CRISM data indicate that the smoothest areas of the youngest crater floor units stand out as having clear signatures of high-calcium pyroxene (HCP). These areas that are proximal to the delta scarp are also delta-like in CRISM low-calcium pyroxene (LCP) spectral signature.
6. Compared to surrounding crater floor terrain, LCP absorptions are deeper in Us material near the western delta front and surrounding the eastern delta remnants. Similarly strong LCP absorptions are also present on the western delta surface. This observed distribution is consistent with LCP-bearing Us material in the crater floor assemblage being derived from or preserved by overlying deltaic material.
7. The HCP signatures of the broader crater floor region correspond to a clearly arcuate region of low thermal inertia that appears to possibly correspond with Us and, based on the arcuate shape, to the past extent of the youngest delta deposits.
8. Finally, we have also estimated the past minimum extent of the western delta in Jezero to have extended further out compared to the present extent. This area corresponds to, at least, the smoothest area of the Us, indicating that the scarcity of impact craters on the underlying unit near the delta is due to recent coverage.

A scenario where a portion or all of the western delta postdates deposition of the youngest crater floor unit(s) cannot be ruled out on the basis of results of crater counting on the delta and the floor because of the limited area of the delta. In addition, the Cf-fr unit may have been protected from impact cratering during period(s) since its formation.

Crater-fill deposits in Jezero were deposited during a complex history with multiple fluvial episodes, and the rocks do not only have great potential to shed light on the geologic evolution of Mars, but also hold key information on the evolution of the early Martian climate, surface environments, and habitability.

Data Availability Statement

Maps of fractures and small craters reported in this work are available through Holm-Alwmark et al. (2021). For HiRISE mosaic of Jezero crater, see Ferguson, Galuszka, et al. (2020). For data used to produce the DEM (Figure 6), see Ferguson, Hare, et al. (2020), Malin et al. (2007); https://astrogeology.usgs.gov/search/map/Mars/Mars2020/JEZ_ctx_B_soc_008_DTM_MOLAtopography_DeltaGeoid_20m_Eqc_latTs0_lon0. CAMP source files “Web-based Spatial Data Infrastructure for Planetary Science Operations” are available on GitHub at <https://github.com/NASA-AMMOS/MMGIS>.

Acknowledgments

Danish participation in the Mars 2020 project was supported by the Carlsberg Foundation grant CF19-0023. S. Holm-Alwmark is supported by an International Postdoc grant from the Swedish Research Council (Grant 2017-06388). J. D. Tarnas was supported by a NASA Postdoctoral Fellowship. The authors want to thank H. Dypvik and S. Ruff for insightful discussions. We also want to thank D. Tirsch for help with the preparation of Figure 1b. Finally, the authors acknowledge thorough and constructive reviews by N. Warner, F. Salese, and one anonymous reviewer, as well as professional editorial handling by D. Rogers.

References

- Baker, V. R., & Partridge, J. B. (1986). Small Martian valleys: Pristine and degraded morphology. *Journal of Geophysical Research*, *91*, 3561–3572. <https://doi.org/10.1029/JB091iB03p03561>
- Bramble, M. S., Mustard, J. F., & Salvatore, M. R. (2017). The geological history of Northeast Syrtis Major, Mars. *Icarus*, *293*, 66–93. <https://doi.org/10.1016/j.icarus.2017.03.030>
- Brown, A. J., Viviano, C. E., & Goudge, T. A. (2020). Olivine-carbonate mineralogy of the Jezero crater region. *Journal of Geophysical Research: Planets*, *125*, e2019JE006011. <https://doi.org/10.1029/2019JE006011>
- Calef, F. J. III, Abarca, H. E., Soliman, T., Abercrombie, S. P., & Powell, M. W. (2019). Multi-mission geographic information system: An open source solution for planetary science operations. Paper presented at 4th Planetary Data Workshop, Flagstaff, AZ, Abstract #7071.
- Calef, F. J., Newsom, H., Williams, J., Parker, T. J., Lamb, M., & Grotzinger, J. (2016). Gale crater morphology compared to other high central peak craters on Mars. Paper presented at 47th Lunar and Planetary Science Conference, Houston, TX, Abstract #2822.
- Carr, M. H., & Head, J. W. III (2003). Oceans on Mars: An assessment of the observational evidence and possible fate. *Journal of Geophysical Research*, *108*(E5), 5042. <https://doi.org/10.1029/2002JE001963>
- Chapman, M. G., Neukum, G., Dumke, A., Michael, G., van Gasselt, S., Kneissl, T., et al. (2010). Noachian-Hesperian geologic history of the Echus Chasma and Kasei Valles system on Mars: New data and interpretations. *Earth and Planetary Science Letters*, *294*, 256–271. <https://doi.org/10.1016/j.epsl.2009.11.032>
- Craddock, R. A., & Howard, A. D. (2002). The case for rainfall on a warm, wet early Mars. *Journal of Geophysical Research*, *107*(E11), 5111. <https://doi.org/10.1029/2001JE001505>
- Davis, J. M., Balme, M., Grindrod, P. M., Williams, R. M. E., & Gupta, S. (2016). Extensive Noachian fluvial systems in Arabia Terra: Implications for early Martian climate. *Geology*, *44*, 847–850. <https://doi.org/10.1130/G38247.1>
- Day, M., & Dorn, T. (2019). Wind in Jezero crater, Mars. *Geophysical Research Letters*, *46*, 3099–3107. <https://doi.org/10.1029/2019GL082218>
- Edgett, K. S., Edgar, L. A., House, C. H., Grotzinger, J. P., Bennett, K. A., Newsom, H. E., et al. (2018). Multi-cycle sedimentary rocks on Mars and implications. Paper presented at 49th Lunar and Planetary Science Conference, Houston, TX, Abstract #1669.
- Ehlmann, B. L., Mustard, J. F., Fassett, C. I., Schon, S. C., Head, J. W. III, Des Marais, D. J., et al. (2008). Clay minerals in delta deposits and organic preservation potential on Mars. *Nature Geoscience*, *1*, 355–358. <https://doi.org/10.1038/ngeo207>
- Ehlmann, B. L., Mustard, J. F., Murchie, S. L., Poulet, F., Bishop, J. L., Brown, A. J., et al. (2008). Orbital identification of carbonate-bearing rocks on Mars. *Science*, *322*, 1828–1832. <https://doi.org/10.1126/science.1164759>
- Ehlmann, B. L., Mustard, J. F., Swayze, G. A., Clark, R. N., Bishop, J. L., Pule, F., et al. (2009). Identification of hydrated silicate minerals on Mars using MRO-CRISM: Geologic context near Nili Fossae and implications for aqueous alteration. *Journal of Geophysical Research*, *114*, E00D08. <https://doi.org/10.1029/2009JE003339>
- Farley, K. A., Williford, K. M., Stack, K. M., Bhartia, R., Chen, A., de la Torre, M., et al. (2020). Mars 2020 mission overview. *Space Science Reviews*, *216*, 142. <https://doi.org/10.1007/s11214-020-00762-y>
- Fassett, C. I., & Head, J. W. III (2005). Fluvial sedimentary deposits on Mars: Ancient deltas in a crater lake in the Nili Fossae region. *Geophysical Research Letters*, *32*, L14201. <https://doi.org/10.1029/2005GL023456>
- Fassett, C. I., & Head, J. W. III (2008a). The timing of Martian valley network activity: Constraints from buffered crater counting. *Icarus*, *195*, 61–89. <https://doi.org/10.1016/j.icarus.2007.12.009>
- Fassett, C. I., & Head, J. W. III (2008b). Valley network-fed, open-basin lakes on Mars: Distribution and implications for Noachian surface and subsurface hydrology. *Icarus*, *198*, 37–56. <https://doi.org/10.1016/j.icarus.2008.06.016>
- Ferguson, R. L., Christensen, P. R., & Kieffer, H. H. (2006). High-resolution thermal inertia derived from the thermal emission imaging system (THEMIS): Thermal model and applications. *Journal of Geophysical Research*, *111*, E12004. <https://doi.org/10.1029/2006JE002735>
- Ferguson, R. L., Galuszka, D. M., Hare, T. M., Mayer, D. P., & Redding, B. L. (2020). Mars 2020 terrain relative navigation HiRISE orthorectified image mosaic [data set]. U.S. Geological Survey. <https://doi.org/10.5066/P9QJDP48>
- Ferguson, R. L., Hare, T. M., Mayer, D. P., Galuszka, D. M., Redding, B. L., Smith, E. D., et al. (2020). Mars 2020 terrain relative navigation flight product generation: Digital terrain model and orthorectified image mosaics. Paper presented at 51st Lunar and Planetary Science Conference, Houston, TX, Abstract #2020.
- Garvin, J. B., Sakimoto, S. E. H., & Frawley, J. J. (2003). Craters on Mars: Global geometric properties from gridded MOLA topography. Paper presented at Sixth International Conference on Mars, Pasadena, CA, Abstract #3277.

- Goddard, K., Warner, N. H., Gupta, S., & Kim, J. R. (2014). Mechanisms and timescales of fluvial activity at Mojave and other young Martian craters. *Journal of Geophysical Research: Planets*, *119*, 604–634. <https://doi.org/10.1002/2013JE004564>
- Goehring, L. (2013). Evolving fracture patterns: Columnar joints, mud cracks and polygonal terrain. *Philosophical Transactions of the Royal Society A*, *371*, 20120353. <https://doi.org/10.1098/rsta.2012.0353>
- Golder, K., Miklusiac, N., Spaulding, R., Atkins, J., Hicks, T., Shaver, E., & Kah, L. (2020). Behavioral characteristics of dark-toned crater floor materials, Jezero crater: Implications for mode of emplacement. Paper presented at 51st Lunar and Planetary Science Conference, Houston, TX, Abstract #1302.
- Golder, K. B., Burr, D. M., & Kattenhorn, S. A. (2020). Investigation of target property effects on crater populations in long lava flows: A study in the Cerberus region, Mars, with implications for magma source identification. *Icarus*, *335*, 113388. <https://doi.org/10.1016/j.icarus.2019.113388>
- Golombek, M. P., & Bridges, N. T. (2000). Erosion rates on Mars and implications for climate change: Constraints from the Pathfinder landing site. *Journal of Geophysical Research*, *105*, 1841–1853. <https://doi.org/10.1029/1999JE001043>
- Golombek, M. P., Grant, J. A., Crumpler, L. S., Greeley, R., Arvidson, R. E., Bell, J. F. III, et al. (2006). Erosion rates at the Mars exploration rover landing sites and long-term climate change on Mars. *Journal of Geophysical Research*, *111*, E12S10. <https://doi.org/10.1029/2006JE002754>
- Goudge, T. A., Head, J. W., Mustard, J. F., & Fassett, C. I. (2012). An analysis of open-basin Lake deposits on Mars: Evidence for the nature of associated lacustrine deposits and post-lacustrine modification processes. *Icarus*, *219*, 211–229. <https://doi.org/10.1016/j.icarus.2012.02.027>
- Goudge, T. A., Milliken, R. E., Head, J. W., Mustard, J. F., & Fassett, C. I. (2017). Sedimentological evidence for a deltaic origin of the western fan deposit in Jezero crater, Mars and implications for future exploration. *Earth and Planetary Science Letters*, *458*, 357–365. <https://doi.org/10.1016/j.epsl.2016.10.056>
- Goudge, T. A., Mohrig, D., Cardenas, B. T., Hughes, C. M., & Fassett, C. I. (2018). Stratigraphy and paleohydrology of delta channel deposits, Jezero crater, Mars. *Icarus*, *301*, 58–75. <https://doi.org/10.1016/j.icarus.2017.09.034>
- Goudge, T. A., Mustard, J. F., Head, J. W., Fassett, C. I., & Wiseman, S. M. (2015). Assessing the mineralogy of the watershed and fan deposits of the Jezero crater paleolake system, Mars. *Journal of Geophysical Research: Planets*, *120*, 775–808. <https://doi.org/10.1002/2014JE004782>
- Grant, J. A., & Schultz, P. H. (1990). Gradational epochs on Mars: Evidence from west-northwest Isidis Basin and Electris. *Icarus*, *84*, 166–195. [https://doi.org/10.1016/0019-1035\(90\)90164-5](https://doi.org/10.1016/0019-1035(90)90164-5)
- Grau Galofre, A., Jellinek, A. M., & Osinski, G. R. (2020). Valley formation on early Mars by subglacial and fluvial erosion. *Nature Geoscience*, *13*, 663–668. <https://doi.org/10.1038/s41561-020-0618-x>
- Grotzinger, J. P., Gupta, S., Malin, M. C., Rubin, D. M., Schieber, J., Siebach, K., et al. (2015). Deposition, exhumation, and paleoclimate of an ancient lake deposit, Gale crater, Mars. *Science*, *350*, aac7575. <https://doi.org/10.1126/science.aac7575>
- Grotzinger, J. P., Sumner, D. Y., Kah, L. C., Stack, K., Gupta, S., Edgar, L., et al. (2013). A Habitable fluvio-lacustrine environment at Yellowknife Bay, Gale Crater, Mars. *Science*, *343*, 1242777. <https://doi.org/10.1126/science.1242777>
- Gudmundsson, A. (2011). *Rock fractures in geological processes* (p. 578). Cambridge, UK: Cambridge University Press. <https://doi.org/10.1017/CBO9780511975684>
- Gudmundsson, A., & Brenner, S. L. (2001). How hydrofractures become arrested. *Terra Nova*, *13*, 456–462. <https://doi.org/10.1046/j.1365-3121.2001.00380.x>
- Gudmundsson, A., Fjeldskaar, I., & Brenner, S. L. (2002). Propagation pathways and fluid transport of hydrofractures in jointed and layered rocks in geothermal fields. *Journal of Volcanology and Geothermal Research*, *116*, 257–278. [https://doi.org/10.1016/S0377-0273\(02\)00225-1](https://doi.org/10.1016/S0377-0273(02)00225-1)
- Gulick, V. C. (1998). Magmatic intrusions and a hydrothermal origin for fluvial valleys on Mars. *Journal of Geophysical Research*, *103*, 19365–19387. <https://doi.org/10.1029/98JE01321>
- Gulick, V. C., & Baker, V. R. (1990). Origin and evolution of valleys on Martian volcanoes. *Journal of Geophysical Research*, *95*, 14325–14344. <https://doi.org/10.1029/JB095iB09p14325>
- Hartmann, W. K., Anguita, J., de la Casa, M. A., Berman, D. C., & Ryan, E. V. (2001). Martian cratering 7: The role of impact gardening. *Icarus*, *149*, 37–53. <https://doi.org/10.1006/icar.2000.6532>
- Hauber, E., Platz, T., Reiss, D., Le Deit, L., Kleinhans, M. G., Marra, W. A., et al. (2013). Asynchronous formation of Hesperian and Amazonian-aged deltas on Mars and implications for climate. *Journal of Geophysical Research: Planets*, *118*, 1529–1544. <https://doi.org/10.1002/jgre.20107>
- Hauber, E., van Gasselt, S., Chapman, M. G., & Neukum, G. (2008). Geomorphic evidence for former lobate debris aprons at low latitudes on Mars: Indicators of the Martian paleoclimate. *Journal of Geophysical Research*, *113*, E02007. <https://doi.org/10.1029/2007JE002897>
- Head, J. (2007). The geology of Mars: New insights and outstanding questions. In M. Chapman (Ed.), *The geology of Mars: Evidence from Earth-based analogs* (pp. 1–46). Cambridge, UK: Cambridge University Press. <https://doi.org/10.1017/CBO9780511536014.002>
- Herd, C. D. K., Bosak, T., Stack, K. M., Sun, V. Z., Benison, K. C., Cohen, B. A., et al. (2021). Sampling Mars: Notional caches from Mars 2020 strategic planning. Paper presented at 52nd Lunar and Planetary Science Conference, Houston, TX, Abstract #1987.
- Hoke, M. R. T., & Hynek, B. M. (2009). Roaming zones of precipitation on ancient Mars as recorded in valley networks. *Journal of Geophysical Research*, *114*, E08002. <https://doi.org/10.1029/2008JE003247>
- Holm-Alwmark, S., Kinch, K. M., Hansen, M. D., Shahrzad, S., Svennevig, K., & Abbey, W. J. (2021). *Data Repository: Stratigraphic relationships in Jezero crater, Mars—Constraints on the timing of fluvial-lacustrine activity from orbital observations*. Harvard Dataverse. <https://doi.org/10.7910/DVN/DGMT4H>
- Holo, S. J., & Kite, E. S. (2017). Incision of the Jezero Crater outflow channel by fluvial sediment transport. Paper presented at Fourth International Conference on Early Mars: Geologic, Hydrologic, and Climatic Evolution and the Implications for Life, Flagstaff, AZ, Abstract ID 3007.
- Horgan, B. H. N., Anderson, R. B., Dromart, G., Amador, E. S., & Rice, M. S. (2020). The mineral diversity of Jezero crater: Evidence for possible lacustrine carbonates on Mars. *Icarus*, *339*, 113526. <https://doi.org/10.1016/j.icarus.2019.113526>
- Howard, A. D., Moore, J. M., & Irwin, R. P. III. (2005). An intense terminal epoch of widespread fluvial activity on early Mars: 1. Valley network incision and associated deposits. *Journal of Geophysical Research*, *110*, E12S14. <https://doi.org/10.1029/2005JE002459>
- Hundal, C. B., Mustard, J. F., & Kremer, C. H. (2020). Origin of the pitted capping unit IN NILI FOSSAE, MARS. Paper presented at the 51st Lunar and Planetary Science Conference, Abstract #1629.
- Hynek, B. M., Beach, M., & Hoke, M. R. T. (2010). Updated global map of Martian valley networks and implications for climate and hydrologic processes. *Journal of Geophysical Research*, *115*, E09008. <https://doi.org/10.1029/2009JE003548>

- Irwin, R. P. III, Craddock, R. A., & Howard, A. D. (2005). Interior channels in Martian valley networks: Discharge and runoff production. *Geology*, 33, 489–492. <https://doi.org/10.1130/G21333.1>
- Irwin, R. P. III, Howard, A. D., Craddock, R. A., & Moore, J. M. (2005). An intense terminal epoch of widespread fluvial activity on early Mars: 2. Increased runoff and paleolake development. *Journal of Geophysical Research*, 110, E12S15. <https://doi.org/10.1029/2005JE002460>
- Jaeger, W. L., Keszthelyi, L., Skinner, J. A. Jr., Milazzo, M. P., McEwen, A. S., Titus, T. N., et al. (2010). Emplacement of the youngest flood lava on Mars: A short, turbulent story. *Icarus*, 205, 230–243. <https://doi.org/10.1016/j.icarus.2009.09.011>
- Kah, L., Scheller, E., Eide, S., Meyen, E., Jacob, S., Spaulding, R., et al. (2020). Depositional relationships between crater floor materials in Jezero crater, Mars. Paper presented at 51st Lunar and Planetary Science Conference, Houston, TX, Abstract #1301.
- Keszthelyi, L., McEwen, S., & Thordarson, T. (2000). Terrestrial analogs and thermal models for Martian flood lavas. *Journal of Geophysical Research*, 105, 15027–15049. <https://doi.org/10.1029/1999JE001191>
- Kite, E. S. (2019). Geologic constraints on early Mars climate. *Space Science Reviews*, 215, 10. <https://doi.org/10.1007/s11214-018-0575-5>
- Kite, E. S., Mayer, D. P., Wilson, S. A., Davis, J. M., Lucas, A. S., & Stucky de Quay, G. (2019). Persistence of intense, climate-driven runoff late in Mars history. *Science Advances*, 5, eaav7710. <https://doi.org/10.1126/sciadv.aav7710>
- Kite, E. S., Sneed, J., Mayer, D. P., & Wilson, S. A. (2017). Persistent or repeated surface habitability on Mars during the late Hesperian—Amazonian. *Geophysical Research Letters*, 44, 3991–3999. <https://doi.org/10.1002/2017GL072660>
- Knade, J., Hauber, E., Platz, T., Le Deit, L., & Kinch, K. (2017). Detailed geological mapping of the fluvial deposits in Magong crater, Xanthe Terra, Mars. Paper presented at European Planetary Science Congress, Riga, Latvia, Abstract ID 11.
- Kneissl, T., van Gasselt, S., & Neukum, G. (2011). Map-projection-independent crater size-frequency determination in GIS environments—New software tool for ArcGIS. *Planetary and Space Science*, 59, 1243–1254. <https://doi.org/10.1016/j.pss.2010.03.015>
- Kremer, C. H., Mustard, J. F., & Bramble, M. S. (2019). A widespread olivine-rich ash deposit on Mars. *Geology*, 47, 677–681. <https://doi.org/10.1130/G45563.1>
- Kronyak, R. E., Kah, L. C., Edgett, K. S., VanBommel, S. J., Thompson, L. M., Wiens, et al. (2019). Mineral-filled fractures as indicators of multigenerational fluid flow in the Pahrump Hills Member of the Murray Formation, Gale crater, Mars. *Earth and Space Science*, 6, 238–265. <https://doi.org/10.1029/2018EA000482>
- Kronyak, R. E., Kah, L. C., Miklusicak, N. B., Edgett, K. S., Sun, V. Z., Bryk, A. B., et al. (2019). Extensive polygonal fracture network in s-car point group strata: Fracture mechanisms and implications for fluid circulation in gale crater, Mars. *Journal of Geophysical Research: Planets*, 124, 2613–2634. <https://doi.org/10.1029/2019JE006125>
- Kukkonen, S., & Kostama, V.-P. (2018). Usability of small impact craters on small surface areas in crater count dating: Analysing examples from the Harmakhis Vallis outflow channel, Mars. *Icarus*, 305, 33–49. <https://doi.org/10.1016/j.icarus.2018.01.004>
- Lapôte, M. G. A., & Ielpi, A. (2020). The pace of fluvial meanders on mars and implications for the western delta deposits of Jezero crater. *AGU Advances*, 1, e2019AV000141. <https://doi.org/10.1029/2019AV000141>
- Malin, M. C., Bell, J. F. III, Cantor, B. A., Caplinger, M. A., Calvin, W. M., Clancy, R. T., et al. (2007). Context Camera Investigation on board the Mars Reconnaissance Orbiter. *Journal of Geophysical Research*, 112, E05S04. <https://doi.org/10.1029/2006JE002808>
- Malin, M. C., & Edgett, K. S. (2000). Sedimentary rocks of early Mars. *Science*, 290, 1927–1937. <https://doi.org/10.1126/science.290.5498.1927>
- Malin, M. C., & Edgett, K. S. (2001). Mars global surveyor mars orbiter camera: Interplanetary cruise through primary mission. *Journal of Geophysical Research*, 106, 23429–23570. <https://doi.org/10.1029/2000JE001455>
- Mandl, G. (2005). *Rock joints: The mechanical genesis*. Berlin, Germany: Springer.
- Mandon, L., Quantin-Nataf, C., Thollot, P., Mangold, N., Lozac'h, L., Dromart, G., et al. (2020). Refining the age, emplacement and alteration scenarios of the olivine-rich unit in the Nili Fossae region, Mars. *Icarus*, 336, 113436. <https://doi.org/10.1016/j.icarus.2019.113436>
- Mangold, N. (2012). Fluvial landforms on fresh ejecta craters. *Planetary and Space Science*, 62, 69–85. <https://doi.org/10.1016/j.pss.2011.12.009>
- Mangold, N., Ansan, V., Masson, P., Quantin, C., & Neukum, G. (2008). Geomorphic study of fluvial landforms on the northern Valles Marineris plateau, Mars. *Journal of Geophysical Research*, 113, E08009. <https://doi.org/10.1029/2007JE002985>
- Mangold, N., Dromart, G., Ansan, V., Salese, F., Kleinhans, M. G., Massé, M., et al. (2020). Fluvial regimes, morphometry, and age of Jezero crater paleolake inlet valleys and their exobiological significance for the 2020 rover mission landing site. *Astrobiology*, 20, 994–1013. <https://doi.org/10.1089/ast.2019.2132>
- Mangold, N., Loizeau, D., Poulet, F., Ansan, V., Baratoux, D., LeMouelic, S., et al. (2010). Mineralogy of recent volcanic plains in the Tharsis region, Mars, and implications for platy-ridged flow composition. *Earth and Planetary Science Letters*, 294, 440–450. <https://doi.org/10.1016/j.epsl.2009.07.036>
- Mangold, N., Poulet, F., Mustard, J. F., Bibring, J.-P., Gondet, B., Langevin, Y., et al. (2007). Mineralogy of the Nili Fossae region with OMEGA/Mars Express data: 2. Aqueous alteration of the crust. *Journal of Geophysical Research*, 112, E08S04. <https://doi.org/10.1029/2006JE002835>
- Manville, V. K., Németh, K., & Kano, K. (2009). Source to sink: A review of three decades of progress in the understanding of volcanoclastic processes, deposits, and hazards. *Sedimentary Geology*, 220, 136–161. <https://doi.org/10.1016/j.sedgeo.2009.04.022>
- Marchi, S. (2021). A new Martian crater chronology: Implications for Jezero crater. *The Astronomical Journal*, 161, 187. <https://doi.org/10.3847/1538-3881/abe417>
- McEwen, A., Hansen, C., Bridges, N., Delamere, W. A., Eliason, E., Grant, J., et al. (2003). MRO's High Resolution Imaging Science Experiment (HiRISE): Science expectations. Paper presented at Sixth International Conference on Mars, Pasadena, CA, Abstract #3217.
- Miklusicak, N., Atkins, J., Boring, B., Hicks, T., Shaver, E., Spaulding, R., et al. (2020). Large fractures in Jezero crater: Implications for understanding dark-toned crater floor materials. Paper presented at 51st Lunar and Planetary Science Conference, Houston, TX, Abstract #1303.
- Morgan, G. A., & Head, J. W. (2009). Sinton crater, Mars: Evidence for impact into a plateau icefield and melting to produce valley networks at the Hesperian–Amazonian boundary. *Icarus*, 202, 39–59. <https://doi.org/10.1016/j.icarus.2009.02.025>
- Mustard, J. F., Poulet, F., Gendrin, A., Bibring, J.-P., Langevin, Y., Gondet, B., et al. (2005). Olivine and pyroxene diversity in the crust of Mars. *Science*, 307, 1594–1597. <https://doi.org/10.1126/science.1109098>
- Osinski, G. R., Grieve, R. A. F., Bleacher, J., Neish, C. D., Pilles, E. A., & Tornabene, L. L. (2018). Igneous rocks formed by hypervelocity impact. *Journal of Volcanology and Geothermal Research*, 353, 25–54. <https://doi.org/10.1016/j.jvolgeores.2018.01.015>
- Palucis, M. C., Jasper, J., Garczynski, B., & Dietrich, W. E. (2020). Quantitative assessment of uncertainties in modeled crater retention ages on Mars. *Icarus*, 341, 113623. <https://doi.org/10.1016/j.icarus.2020.113623>
- Palumbo, A. M., Head, J. W., & Wilson, L. (2020). Rainfall on Noachian Mars: Nature, timing, and influence on geologic processes and climate history. *Icarus*, 347, 113782. <https://doi.org/10.1016/j.icarus.2020.113782>

- Peacock, D. C. P., Sanderson, D. J., & Rotevatn, A. (2018). Relationships between fractures. *Journal of Structural Geology*, *106*, 41–53. <https://doi.org/10.1016/j.jsg.2017.11.010>
- Philipp, S. L., Afşar, F., & Gudmundsson, A. (2013). Effects of mechanical layering on hydrofracture emplacement and fluid transport in reservoirs. *Frontiers in Earth Science*, *1*, 1–19. <https://doi.org/10.3389/feart.2013.00004>
- Quantin-Nataf, C., Craddock, R. A., Dubuffet, F., Lozac'h, L., & Martinot, M. (2019). Decline of crater obliteration rates during early Martian history. *Icarus*, *317*, 427–433. <https://doi.org/10.1016/j.icarus.2018.08.005>
- Quantin-Nataf, C., Holm-Alwmark, S., Lasue, J., Calef, F. J., Shuster, D., Kinch, K. M., et al. (2021). The complex exhumation history of Jezero crater floor unit. Paper presented at 52nd Lunar and Planetary Science Conference, Houston, TX, Abstract #2034.
- Ramirez, R. M., Craddock, R. A., & Usui, T. (2020). Climate simulations of early Mars with estimated precipitation, runoff, and erosion rates. *Journal of Geophysical Research: Planets*, *125*, e2019JE006160. <https://doi.org/10.1029/2019JE006160>
- Rogers, A. D., Warner, N. H., Golombek, M. P., Head, J. W. III, & Cowart, J. C. (2018). Areally extensive surface bedrock exposures on Mars: Many are clastic rocks, not lavas. *Geophysical Research Letters*, *45*, 1767–1777. <https://doi.org/10.1002/2018GL077030>
- Ruff, S. W. (2017). Investigating the floor of paleolake Jezero by way of Gusev crater. Paper presented at the Fourth International Conference on Early Mars, Flagstaff, AZ, Abstract #3076.
- Salese, F., Ansan, V., Mangold, N., Carter, J., Ody, A., Poulet, F., et al. (2016). A sedimentary origin for intercrater plains north of the Hellas basin: Implications for climate conditions and erosion rates on early Mars. *Journal of Geophysical Research: Planets*, *121*, 2239–2267. <https://doi.org/10.1002/2016JE005039>
- Salese, F., Di Achille, G., Neesemann, A., Ori, G. G., & Hauber, E. (2016). Hydrological and sedimentary analyses of well-preserved paleofluvial-paleolacustrine systems at Moa Valles, Mars. *Journal of Geophysical Research: Planets*, *121*, 194–232. <https://doi.org/10.1002/2015JE004891>
- Salese, F., Kleinhans, M. G., Mangold, N., Ansan, V., McMahon, W., de Haas, T., & Dromart, G. (2020). Estimated minimum life span of the Jezero fluvial delta (Mars). *Astrobiology*, *20*, 977–993. <https://doi.org/10.1089/ast.2020.2228>
- Salese, F., Mangold, N., Kleinhans, M. G., de Haas, T., Ansan, V., & Dromart, G. (2019). Estimated minimum lifespan of the Jezero crater delta, Mars. Paper presented at 50th Lunar and Planetary Science Conference, Houston, TX, Abstract #2107.
- Salese, F., McMahon, W. J., Balme, M. R., Ansan, V., Davis, J. M., & Kleinhans, M. G. (2020). Sustained fluvial deposition recorded in Mars' Noachian stratigraphic record. *Nature Communications*, *11*, 2067. <https://doi.org/10.1038/s41467-020-15622-0>
- Scheller, E. L., & Ehlmann, B. L. (2020). Composition, stratigraphy, and geological history of the Noachian basement surrounding the Isidis impact basin. *Journal of Geophysical Research: Planets*, *125*, e2019JE006190. <https://doi.org/10.1029/2019JE006190>
- Schon, S. C., Head, J. W., & Fassett, C. I. (2012). An overfilled lacustrine system and progradational delta in Jezero crater, Mars: Implications for Noachian climate. *Planetary and Space Science*, *67*, 28–45. <https://doi.org/10.1016/j.pss.2012.02.003>
- Segura, T. L., Toon, O. B., & Colaprete, A. (2008). Modeling the environmental effects of moderate-sized impacts on Mars. *Journal of Geophysical Research*, *113*, E11007. <https://doi.org/10.1029/2008JE003147>
- Shahrazad, S., Kinch, K. M., Goudge, T. A., Fassett, C. I., Needham, D. H., Quantin-Nataf, C., & Knudsen, C. P. (2019). Crater statistics on the dark-toned, mafic floor unit in Jezero crater, Mars. *Geophysical Research Letters*, *46*, 2408–2416. <https://doi.org/10.1029/2018GL081402>
- Stack, K. M., Edwards, C. S., Grotzinger, J. P., Gupta, S., Sumner, D. Y., Calef, F. J. III, et al. (2016). Comparing orbiter and rover image-based mapping of an ancient sedimentary environment, Aeolis Palus, Gale crater, Mars. *Icarus*, *280*, 3–21. <https://doi.org/10.1016/j.icarus.2016.02.024>
- Stack, K. M., Williams, N. R., Calef, F. J. III, Sun, V. Z., Williford, K. H., Farley, K. A., et al. (2020). Geology of the Mars 2020 landing site, Jezero crater, Mars: Insights from photo-geologic mapping by the Mars 2020 science team. *Space Science Reviews*, *216*, 127. <https://doi.org/10.1007/s11214-020-00739-x>
- Sun, V. Z., & Stack, K. M. (2020a). Geologic map of Jezero Crater and the Nili Planum region, Mars (Map pamphlet 14 p., 1 sheet, scale 1:75,000). U.S. Geological Survey Scientific Investigations. <https://doi.org/10.3133/sim3464>
- Sun, V. Z., & Stack, K. M. (2020b). Geologic map of the Jezero and Nili Planum regions of Mars 2020. Paper presented at Annual Meeting of Planetary Geologic Mappers, Abstract #7019.
- Viviano-Beck, C. E., Seelos, F. P., Murchie, S. L., Kahn, E. L., Seelos, K. D., Taylor, H. W., et al. (2014). Revised CRISM spectral parameters and summary products based on the currently detected mineral diversity on Mars. *Journal of Geophysical Research: Planets*, *119*, 1403–1431. <https://doi.org/10.1002/2014JE004627>
- Warner, N. H., Grant, J. A., Wilson, S. A., Golombek, M. P., DeMott, A., Charalambous, C., et al. (2020). An impact crater origin for the InSight landing site at Homestead hollow, Mars: Implications for near surface stratigraphy, surface processes, and erosion rates. *Journal of Geophysical Research: Planets*, *125*, e2019JE006333. <https://doi.org/10.1029/2019JE006333>
- Warner, N. H., Gupta, S., Calef, F. J. III, Grindrod, P., Boll, N., & Goddard, K. (2015). Minimum effective area for high resolution crater counting of Martian terrains. *Icarus*, *245*, 198–240. <https://doi.org/10.1016/j.icarus.2014.09.024>
- Warner, N. H., Schuyler, A. J., Rogers, A. D., Golombek, M. P., Grant, J., Wilson, S., et al. (2020). Crater morphometry on the mafic floor unit at Jezero crater, Mars: Comparisons to a known basaltic lava plain at the InSight landing site. *Geophysical Research Letters*, *47*, e2020GL089607. <https://doi.org/10.1029/2020GL089607>
- Watkins, J. A., Grotzinger, J., Stein, N., Banham, S. G., Gupta, S., Rubin, D., et al. (2016). Paleotopography of erosional unconformity, base of Stimson formation, Gale crater, Mars. Paper presented at 47th Lunar and Planetary Science Conference, Houston, TX, Abstract #2939.
- Weertman, J. (1980). The stopping of a rising, liquid-filled crack in the Earth's crust by a freely slipping horizontal joint. *Journal of Geophysical Research*, *85*, 967–976. <https://doi.org/10.1029/JB085iB02p00967>
- Werner, S. C. (2008). The early Martian evolution—Constraints from basin formation ages. *Icarus*, *195*, 45–60. <https://doi.org/10.1016/j.icarus.2007.12.008>
- Whitehead, J., Grieve, R. A. F., Garvin, J. B., & Spray, J. G. (2010). The effects of crater degradation and target differences on the morphologies of Martian complex craters. In W. U. Reimold, & R. L. Gibson (Eds.), *Large meteorite impacts and planetary evolution IV* (Vol. 465, pp. 67–80). Geological Society of America Special Paper. [https://doi.org/10.1130/2010.2465\(05\)](https://doi.org/10.1130/2010.2465(05))